Late middle Miocene Metatheria (Mammalia: Didelphimorphia and Paucituberculata) from Juan Guerra, San Martín Department, Peruvian Amazonia

Narla S Stutz, M. Alejandra Abello, Laurent Marivaux, Myriam Boivin, François Pujos, Aldo Marcelo Benites Palomino, Rodolfo Salas-Gismondi, Julia V Tejada-Lara, Michele Andriolli Custódio, Martin Roddaz, et al.

Journal of South American Earth Science (https://doi.org/10.1016/j.jsames.2022.103902)

Late middle Miocene Metatheria (Mammalia: Didelphimorphia and Paucituberculata) from Juan Guerra, San Martín Department, Peruvian Amazonia

Narla S. Stutz[1,2*]; María Alejandra Abello[3]; Laurent Marivaux[2]; Myriam Boivin[4]; François Pujos[5]; Aldo M. Benites-Palomino[6,7]; Rodolfo Salas-Gismondi[7,8]; Julia V. Tejada-Lara[9]; Michele Andriolli Custódio[10,11,12]; Martin Roddaz[11,12]; Roberto Ventura Santos[11]; Ana Maria Ribeiro[1,13]; Pierre-Olivier Antoine[2]

[1]Programa de Pós-Graduação em Geociências, Universidade Federal do Rio Grande do Sul (PPGGEO UFRGS), Avenida Bento Gonçalves, 9500, 91501-970, Porto Alegre, Brazil

[2]Laboratoire de Paléontologie, Institut des Sciences de l'Évolution de Montpellier (ISEM, UMR 5554, UM/CNRS/IRD/EPHE), Université de Montpellier, Place Eugène Bataillon, 34095, Montpellier, France

[3]Unidades de Investigación Anexo Museo, Facultad de Ciencias Naturales y Museo (UNLP), Avenida 60 y 122, B1900FWA, La Plata, Argentina

[4]Instituto de Ecorregiones Andinas (INECOA), Universidad Nacional de Jujuy, CONICET, IdGyM, Avenida Bolivia 1661, 4600, San Salvador de Jujuy, Argentina

[5]Instituto Argentino de Nivología, Glaciología y Ciencias Ambientales (IANIGLA), CCT–CONICET–Mendoza, Avenida Ruiz Leal s/n, Parque Gral. San Martín, 5500, Mendoza, Argentina

[6]c, Universität Zürich, Karl-Schmid-Strasse 4, 8006, Zürich, Switzerland

[7]Departamento de Paleontología de Vertebrados, Museo de Historia Natural - Universidad Nacional Mayor San Marcos (UNMSM, DPV-MUSM), Avenida Arenales 1256, Lima 14, Peru

[8]BioGeoCiencias Lab, Facultad de Ciencias y Filosofía/CIDIS, Laboratorios de Investigacion y Desarrollo (LID), Centro de Investigación para el Desarrollo Integral y Sostenible (CIDIS), Universidad Peruana Cayetano Heredia, Avenida Honorio Delgado 430, Lima 31, Peru

[9]Department of Archaeology, University of Cambridge, Downing Street, CB2 3DZ, Cambridge, England.

[10]Instituto de Ciências Exatas, Departamento de Geociências, Universidade Federal do Amazonas (UFAM), Avenida General Rodrigo Octavio Jordão Ramos, 1200, Coroado I, 69067-005, Manaus, Brazil

[11]Laboratório de Geocronologia, Instituto de Geociências, Universidade de Brasília (UnB), Campus Universitário Darcy Ribeiro ICC - Ala Central, 70910-000, Brasília, Brazil

[12]Géosciences-Environnement Toulouse, Université de Toulouse (UPS (SVT-OMP)/CNRS/IRD), 14 Avenue Édouard Belin, F-31400, Toulouse, France

[13]Seção de Paleontologia, Museu de Ciências Naturais, Secretaria do Meio Ambiente e Infraestrutura, Avenida Dr. Salvador França, 1427, 90690-000, Porto Alegre, Brazil

*Corresponding author. *Email address*: narlasstutz@gmail.com (N. Stutz).

Abstract

Currently, marsupials (modern members of the Metatheria clade) are widely distributed in tropical and subtropical areas of South America, but poorly represented in the fossil record of these regions. Except for the species-rich fossiliferous localities of La Venta in Colombia, additional Miocene metatherians from tropical, equatorial South America are sparsely reported in Bolivia, Brazil, Peru, and Venezuela. Here, we introduce new metatherian remains recovered from the late middle Miocene locality of TAR-31, San Martín Department, Peru, which has been assigned to the Laventan South American Land Mammal Age (~13 Ma) by mammalian biostratigraphy. Three metatherian taxa are recognized at TAR-31: the didelphid didelphimorph '*Thylamys*' cf. '*T.*' *colombianus*, and the paucituberculatans aff. *Palaeothentes* and *Pitheculites ipururensis* sp. nov. This assemblage and the presence of a cebid primate at TAR-31 suggests predominantly humid and warm tropical conditions, with the occurrence of both forests and drier habitats in the surroundings. Comparisons with other Miocene metatherian assemblages at low and mid latitudes of South America clearly confirm close relationships between TAR-31 and La Venta (agreeing with observations based on monkeys and rodents), as well as, to a lesser extent, with Acre River local faunas and Madre de Dios (MD-67) in Brazil and Peru, respectively. The current results support the hypothesis that Western Amazonia was a single and consistent biogeographical region for land mammals over middle Miocene times, at the western edge of the Pebas Mega-Wetland System, and highlight the role of the Amazonian region concerning marsupial Neogene radiation. U-Pb analysis made on detrital zircon grains from TAR-31 gave a maximum depositional age of 17.4 ± 0.12 Ma (*i.e.*, 4 Ma older than the biostratigraphical age), with a mixed detrital source likely comprising Precambrian (Western Amazon Craton), Neoproterozoic (Neoproterozoic mobile belts), and Phanerozoic rocks (Andes).

Keywords: Paucituberculata, Didelphimorphia, Laventan, Paleobiogeography, Pebas Mega-Wetland System.

1. Introduction

Western Amazonia has been regarded as an epicenter of biodiversity across the entire Cenozoic era (*e.g.*, Hoorn *et al.*, 2010; Antoine *et al.*, 2016, 2021; Carvalho *et al.*, 2021). In particular, this area hosted a great mammalian diversity during the middle to late Miocene interval (with up to 14 orders and 40 families documented; Antoine *et al.*, 2017). This large diversity in northern South America coincides with a series of geomorphological processes related to the Andean orogeny (Hoorn *et al.*, 2010; Moreno *et al.*, 2020), and with the Miocene Climatic Optimum (**MCO**; Hoorn *et al.*, 2010; Westerhold *et al.*, 2020), which would have promoted the growth of tropical forests (probably present in the area since the Paleocene; Wing *et al.*, 2009; Jaramillo *et al.*, 2010, 2017; Carvalho *et al.*, 2021). Furthermore, between 18 to 10 Ma, Western Amazonia was heavily influenced by the Pebas Mega-Wetland System (**PMWS**), an unparalleled landscape complex with wetlands, swamps, lakes, floodplains, and fluvial systems covering a broad area, fed by water and sediments coming from the Andes, and sporadic marine influence (Hoorn *et al.*, 2010; Boonstra *et al.*, 2015; Antoine *et al.*, 2016; Alvim *et al.*, 2021). This system probably resembled the South American Pantanal in some ways, but differing from it in being considerably larger (Marivaux *et al.*, 2020).

Only a few Miocene fossil mammal-bearing localities are known to depict Miocene faunas at tropical latitudes of South America. These include the Castillo, Querales, Socorro, and Urumaco formations in Venezuela (various localities, early, middle and late Miocene in age; Quiroz and Jaramillo, 2010; Sánchez-Villagra *et al.*, 2010; Rincón *et al.*, 2014; Moreno *et al.*, 2015); Acre basin in Brazil (various localities, late Miocene in age; Negri *et al.*, 2010; Bissaro-Júnior *et al.*, 2019); Madre de Dios (MD-67 locality, early middle Miocene in age; Antoine *et al.*, 2013), Fitzcarrald local fauna (various localities, late middle Miocene in age; Tejada-Lara *et al.*, 2015), Tamshiyacu (late middle Miocene; Salas-Gismondi *et al.*, 2015), Contamana (various localities spanning the early–early late Miocene; Antoine *et al.*, 2016), and Juan Guerra area (locality of TAR-31; Marivaux *et al.*, 2020; Boivin *et al.*, 2021) in Peru; as well as in Colombia with the Castilletes Formation and the outstanding La Venta fauna (Kay *et al.*, 1997; Suárez *et al.*, 2016). The best studied of these fossil communities is La Venta, which is represented by dozens of fossil-bearing localities of the Honda Group at the Magdalena Valley, spanning 13.5–11.6 Ma (*e.g.*, Montes *et al.*, 2021). The La Venta fauna is currently considered the most-diverse and best-documented fossil vertebrate assemblage from the Neotropics (Kay *et al.*, 1997; Croft, 2016; Defler, 2019) and typifies the Laventan South American Land Mammal Age (**SALMA**). The Laventan fauna points to significant

differences between the fossil record at low and mid+high latitudes of South America, including at composition and abundance level (*e.g.*, Kay *et al.*, 1997; Engelman *et al.*, 2015, 2017; Suárez Gómez, 2019).

Nevertheless, several authors (*e.g.*, Flynn *et al.*, 2012; Antoine *et al.*, 2016, 2017; Goin *et al.*, 2016) have noted the poverty of the fossil record of northern South America when compared to that of mid to high latitudes (up to 50° S) of the landmass. Furthermore, among the records already reported for the Amazon region, most of these remains pertain to large eutherian mammals. These biases have long hampered the record and understanding of the paleodiversity and evolution of small mammals, which are the most speciose in Amazonian mammalian guilds (*i.e.*, Metatheria, Chiroptera, Primates, and Rodentia; Antoine *et al.*, 2017; Defler, 2019). The situation has recently changed thanks to new collecting techniques (screen-washing; *e.g.*, Antoine *et al.*, 2016, 2017), allowing for sampling microvertebrates and, among them, micromammals.

Metatheria, whose living representatives are the marsupials (*e.g.*, opossums, shrew opossums, and *monito del monte* in the Americas; kangaroos, koalas, and others in Australasia), are currently distributed in South America mainly in tropical and subtropical areas, but poorly represented in the fossil record of these regions (Goin *et al.*, 2007, 2016; Antoine *et al.*, 2017; Voss and Jansa, 2021). During the Miocene epoch, South American fossil metatherians from low and mid-latitudes are solely reported at Cerdas (a new Borhyaenoidea still to be described, Croft *et al.*, 2016), Quebrada Honda (seven species of three families of three orders; Engelman *et al.*, 2017, 2020), and Achiri (Altiplano, with the sparassodontan *Borhyaenidium altiplanicum*, Villarroel and Marshal, 1983) in Bolivia; Acre, in Brazil (sparse records of didelphids; Czaplewski, 1996; Cozzuol *et al.*, 2006), Urumaco, in Venezuela (one possible record; Linares, 2004); and in Peruvian Amazonia, with didelphids from the Río Acre (Czaplewski, 1996; Goin and de los Reyes, 2011), and new sites recently discovered (up to four species, three families, and three orders; *e.g.*, Madre de Dios, Fitzcarrald local fauna, Contamana, and Tarapoto/Juan Guerra vicinity; Antoine *et al.*, 2013, 2016; Tejada-Lara *et al.*, 2015; Marivaux *et al.*, 2020). Furthermore, in Colombia there are records for the Castilletes Formation (the sparassodontan *Lycopsis padillai*, Suárez *et al.*, 2016) and the La Venta local fauna, in Colombia, which is a striking exception, including 11 species documenting four orders and eight families (Suárez Gómez, 2019).

The present study aims at reporting fossil metatherians recovered from the locality of TAR-31, in Peruvian Amazonia, dated as late middle Miocene (Laventan) in age by mammalian biostratigraphy (Marivaux *et al.*, 2020; Boivin *et al.*, 2021), in order to i) part

address the regional gap of knowledge regarding metatherians, ii) depict local paleoenvironments, and iii) provide paleobiogeographic insights in northern South America during the middle Miocene. Additionally, U-Pb on zircon grains ages were obtained to independently constrain the age and further reveal the provenance of the concerned sediments at a Panamazonian scale.

2. Paleontological background and geological setting

The locality of TAR-31 (6°35.261S, 76°18.347W) is situated at the vicinity of Juan Guerra, near Tarapoto, in the San Martín Department, Peruvian Amazonia. It is located next to the bridge called "*Puente Colombia*", on the left bank of the *Río Mayo* (Figure 1). The fossil-bearing layer is a microconglomerate lens 10 to 15 cm-thick, which was completely mined out, assigned to the lower member of the Ipururo Formation (**Fm**.) (Figure 2; Marivaux *et al*., 2020; Boivin *et al.*, 2021). Fossil specimens documenting a wide array of organisms have been recovered from this locality, such as seeds, silicified wood, amber clasts (with no organic inclusions so far), decapod crustaceans, fishes (Chondrichthyes and Actinopterygii), anurans, turtles, crocodylomorphs, an unidentified bird, and several mammal orders. Among those mammals, the cebid primate *Neosairimi* cf. *fieldsi*, nine rodent taxa, including the octodontoid *Ricardomys longidens*, the chinchilloids *Microscleromys paradoxalis* and *M. cribriphilus*, and the erethizontoid *Nuyuyomys chinqaska* (Marivaux *et al*., 2020; Boivin *et al*., 2021) have already been described in detail. Additionally, the interatheriine notoungulate *Miocochilius* sp., the didolodontid litoptern *Megadolodus* sp., as well as chiropterans, sirenians and xenarthrans have been preliminarily identified. Based on its fauna, TAR-31 was dated as late middle Miocene in age (Laventan; Marivaux *et al*., 2020; Boivin *et al*., 2021) (Figure 2). TAR-31 is further situated stratigraphically ~110 m above another vertebrate locality in the same section (TAR-16, Fig. 2). This latter locality has notably yielded teeth of the giant caimanine *Purussaurus* sp. and dermal scutes of the pampatheriid xenarthran *Scirrotherium* sp., pointing to an early middle–late Miocene age (Jiménez-Lara, 2020), in good agreement with the hypothesized age for TAR-31.

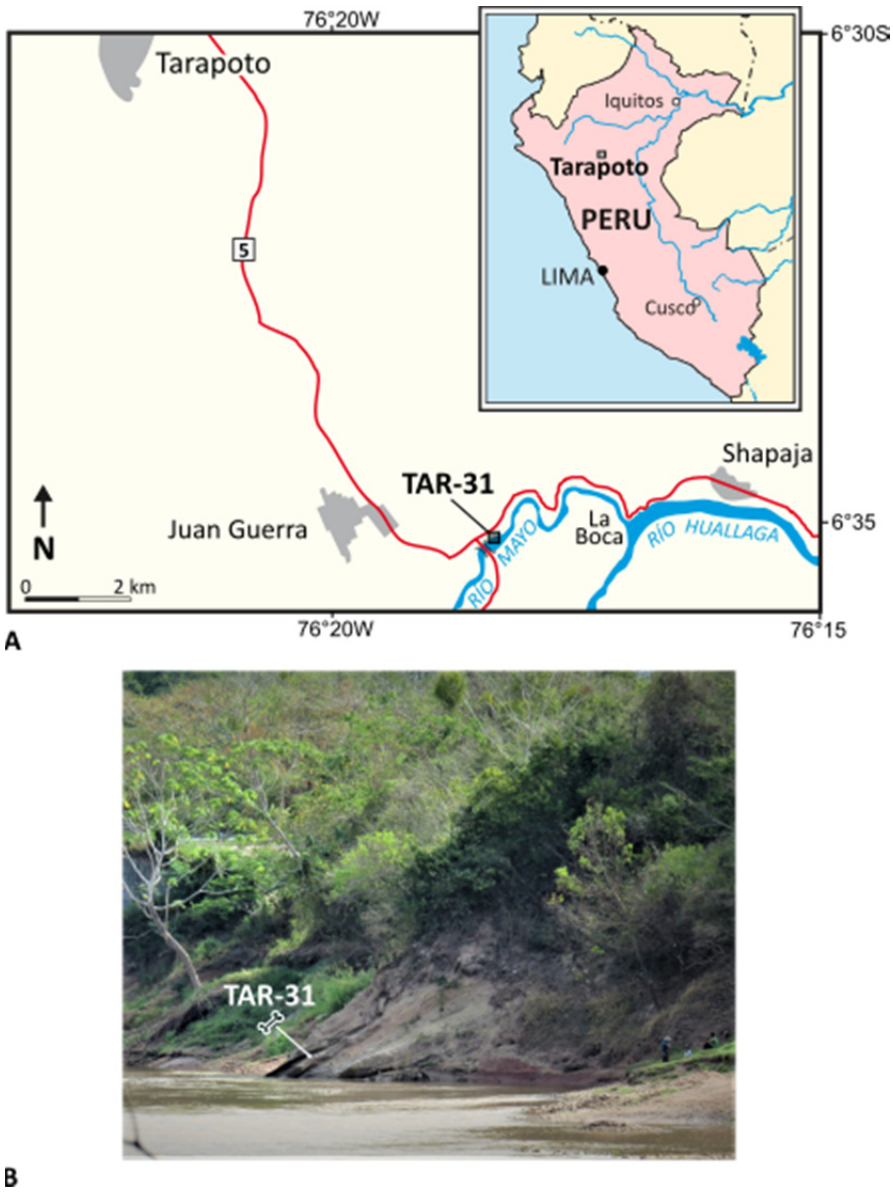

Figure 1. A. Location map of the TAR-31 fossil locality in the Tarapoto/Juan Guerra area, San Martín Department, Peru. **B**. Exposures of the Ipururo Formation along the left bank of the *Río Mayo* during the dry season, with mention of the fossil-yielding level, TAR-31.

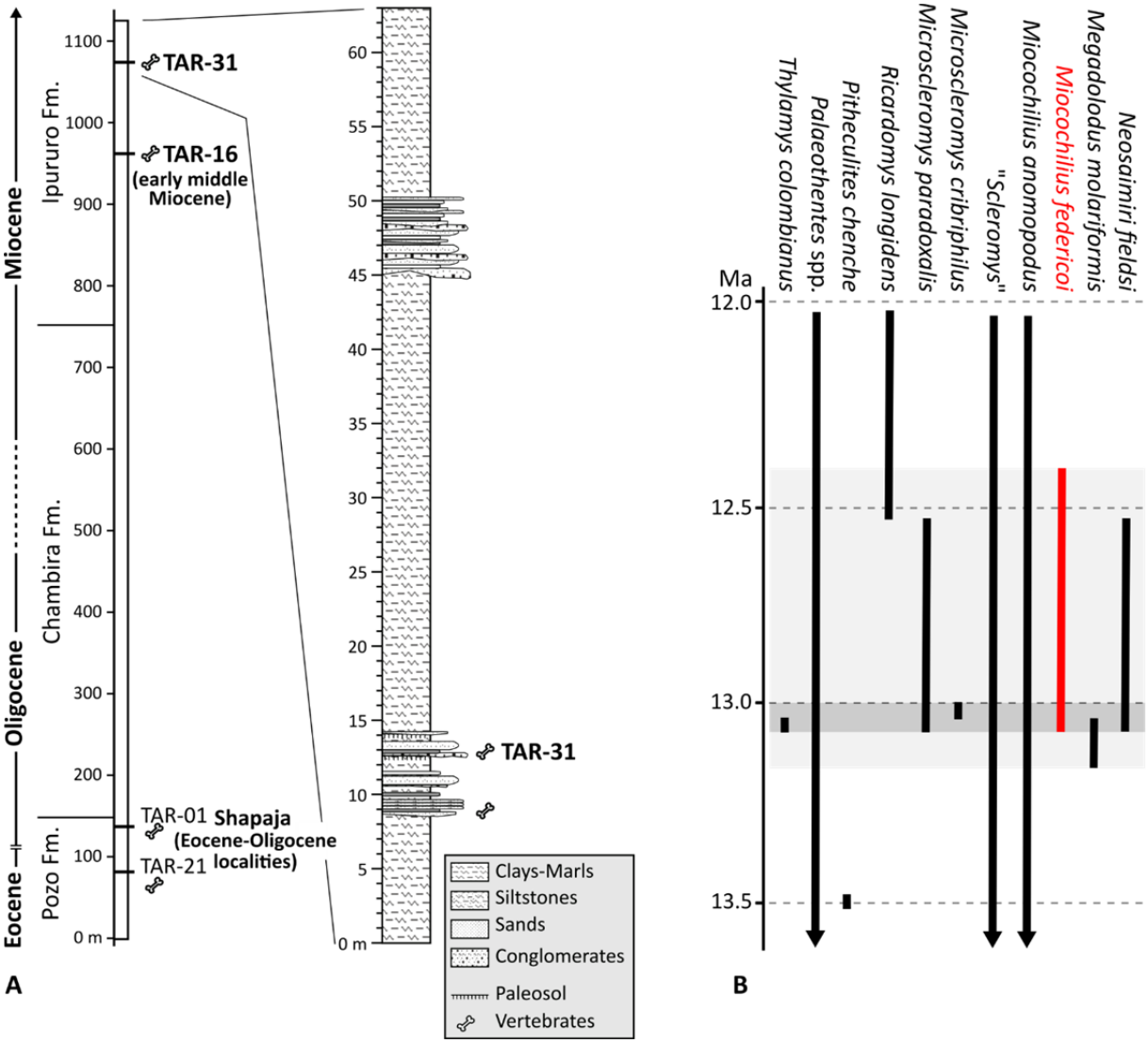

Figure 2. A, Stratigraphic log of the deposits at Juan Guerra, San Martín Department, Peru, including the localities of TAR-31 and TAR-16 and the Shapaja section (see Antoine *et al*., 2021). **B**, Hypothesized age of TAR-31 (dark grey horizontal area), based on biostratigraphical ranges of mammalian taxa of interest (see Marivaux *et al*., 2020, Boivin *et al*., 2021, and references therein). The light grey area encompasses all stratigraphic ranges previously documented for TAR-31 mammals. Abbreviations: Fm., Formation; Lit., Litopterna; Not., Notoungulata; Pr., Primates.

3. Material and Methods

3.1 Material

All the specimens were collected during yearly paleontological field campaigns in 2015–2018, using the screen-washing technique, with meshes of 2 and 1 mm, totaling

approximately 550 kg of sediments treated. The residues of the sieves were then examined under stereomicroscopes for microfossil picking.

The specimens are permanently housed at the Vertebrate Paleontology Department of the *Museo de Historia Natural* of the *Universidad Nacional Mayor San Marcos* (**MUSM**) in Lima, Peru. They were photographed using a Hitachi S 4000 Scanning Electron Microscope (**SEM**) at the *Institut des Neurosciences de Montpellier* (**INM**), France. Dental measurements (*i.e.*, maximum anteroposterior length and maximum labiolingual width) were made using a microscope fitted with a calibrated reticle (Nikon Measuroscope, 1/100 mm).

3.2 Methods

Systematics and description

The systematics follows Goin *et al*. (2016). The taxonomic identifications were made based on Marshall (1976), Dumont and Bown (1997), Goin (1997), Abello (2007), and Engelman *et al*. (2017). Molars were described based on the dental nomenclature and homologies proposed by Abello (2013), Goin *et al*. (2016), and Engelman *et al*. (2017).

Anatomical abbreviations

M, upper molar; **m**, lower molar; **P**, upper premolar; **p**, lower premolar; **StA**–**D**, stylar cusps (from anterior to posterior).

U-Pb dating methods

Sample TAR-31 was prepared and analyzed for U-Pb analyses at the *Laboratório de Estudos Geodinâmicos, Geocronológicos e Ambientais*, *Universidade de Brasília* (LEGGA/UnB). Zircon grains were obtained from the fossil bearing conglomerate of TAR-31 outcrop. Sample processing included crushing followed by heavy minerals concentration by panning and using a Frantz Isodynamic Magnetic Separator to eliminate magnetic mineral grains. Next, the zircon grains were randomly handpicked (~120 grains) under a stereomicroscope microscope and mounted on adhesive tape, enclosed in a 9 mm diameter plastic ring placed on the tape around the zircons. Afterwards, the plastic ring was filled with epoxy resin and once polymerized, it was polished to expose the zircon grains (Gehrels *et al*., 2008; Bühn *et al*., 2009; Gehrels, 2014). After this stage, zircon grains were imaged by SEM back-scattered electron (**BSE**) to identify morphological features, internal structures, and the best area for laser ablation. The U-Pb isotopic analyses on zircon by laser ablation mass spectrometry (**LA-MC-ICP-MS**) followed the procedures of Bühn *et al*. (2009). The effective

U-Pb ages were $^{206}Pb/^{238}U$ ages for zircon grains with ages < 1.0 Ga and $^{207}Pb/2^{06}Pb$ ages for grains with ages > 1.0 Ga.

Based on U-Pb results, we calculated the oldest possible age of the sedimentary deposit, *i.e.*, the maximum depositional age (**MDA**; Dickinson and Gehrels, 2009; Sharman *et al.*, 2018; Sharman and Malkowski, 2020). This is a statistic method that aims to date individual particles of sediment, most notably detrital zircon U-Pb dating via laser ablation mass spectrometry. The application of this method assumes that detrital sedimentary rocks cannot be deposited before their constituent particles are formed, so the youngest particles in a given deposit constrain the MDA (Sharman and Malkowski, 2020). We reported the MDA for the detrital sample selecting at least three analyses in the youngest cluster of ages and, the YC2σ [3+] was defined as the weighted mean average of the three youngest overlapped analyses and associated 2σ uncertainty of this cluster (Dickinson and Gehrels, 2009; Sharman *et al.*, 2018; Sharman and Malkowski, 2020).

4. Results

4.1 U-Pb dating results

Results from the detrital zircon U-Pb analyses of the sample TAR-31 sample are summarized in Figure 3. Analytical results of the 126 dated grains are presented in the Supplementary Data.

The MDA, calculated as the weighted mean of the YC2σ (+3) following Sharman and Malkowski (2020), yielded an age of 17.4 ± 0.12 Ma, which is older than the presumed biostratigraphic age of the sample (see 5.2).

Potential source of the detrital sample includes Precambrian rocks of the Western Amazon Craton, the Neoproterozoic rocks of the Neoproterozoic mobile belts and Andean rocks including Famatinian and Paleozoic magmatic rocks, Permian volcanic rocks (Mitu), and Meso-Cenozoic volcanic rocks of the Andean Arc (Figure 3).

Based on zircon grains U-Pb geochronological ages distribution (Figure 3), the main source areas of the analyzed sedimentary rock were the Rio Negro-Jurena (1.82–1.54 Ga) (7.9%), Rondonia-San Ignácio (1.54–1.3 Ga) (31%), Greenville Sunsás (1.3–0.9 Ga) (14.3%), Brazilian (0.7–0.5 Ga) (11.1%), Paleozoic-Magmatic Arc (0.4–0.26 Ga) (9.5%), and Cenozoic Andean Arc (< 0.065 Ga) (9.5%) terrains. The grains yielded minor peaks of Central Amazon (> 2.2 Ga) (1.6%), Maroni-Itacaiunas (2.2–2 Ga) (2.4%), Ventuari-Tapajós (2–1.82 Ga) (3.2%), Undefined deposits (0.9–0.7 Ga) (3.2%), Famatinian (0.5–0.4 Ga)

(3.2%), Triassic-Jurassic (0.145–0.25 Ga) (1.6%), and Cretaceous Andean Arc (< 0.145 Ga) (1.6%).

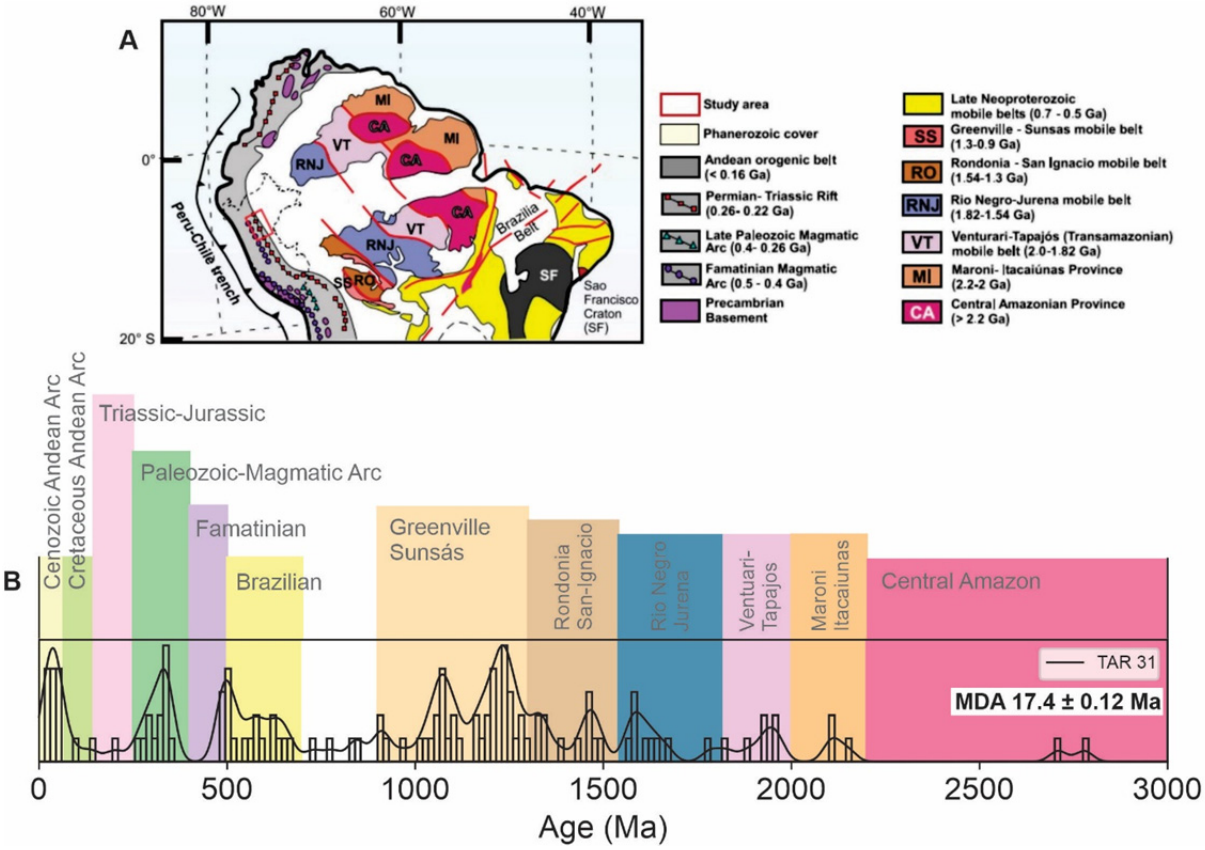

Figure 3. **A**, Sketch map of the northern part of South America illustrating the major tectonic provinces and the ages of their more recent metamorphic events. Modified and adapted from Sato *et al*. (2000), Chew *et al*. (2007, 2008), Bahlburg *et al*. (2009, 2011), Spikings *et al*. (2016), and Hurtado *et al*. (2018). The red rectangle indicates the location of the study area. **B**, Detrital zircon age spectra for the TAR-31 sample and potential corresponding sedimentary sources (identified by colored rectangles, except for undefined deposits).

4.2 Systematic Paleontology

Class Mammalia Linnaeus, 1758

Infraclass Metatheria Huxley, 1880

Supercohort Marsupialia Gill, 1872

Order Didelphimorphia Gill, 1872

Family Didelphidae Gray, 1821

Subfamily Didelphinae Gray, 1821

Tribe Thylamyini Hershkovitz, 1992

Genus '*Thylamys*' Gray, 1843

'*Thylamys*' cf. '*T.*' *colombianus* Goin, 1997

(Figure 4A–C)

Referred material. MUSM 4018, left m1 (Figure 4A–C).

Locality. TAR-31, Juan Guerra, Tarapoto Province, San Martín Department, Peru.

Formation and age. Ipururo Fm., lower member, late middle Miocene (see Marivaux *et al*., 2020).

Measurements. See Table 1.

Description. The trigonid of MUSM 4018 is slightly longer and narrower than the talonid, but generally both parts are subequal in dimensions. The paraconid is located slightly labially to the metaconid. Despite the broken tip, the paraconid seems to have been the lowest trigonid cuspid, much lower than the protoconid and slightly lower than the metaconid, but is still conspicuous. The postparacristid is well-developed and obliquely oriented. A subtle anterior cingulid is present, with a protruding anteriormost portion and an inconspicuous basal portion, but it is worn and partially broken. The protoconid is the highest cuspid of the trigonid and of the molar in general. The preprotocristid is well developed and obliquely oriented towards the notch where it joins the postparacristid, forming a wide obtuse angle. The postprotocristid is shorter than the preprotocristid. It is obliquely and dorso-ventrally oriented and linked to the postmetacristid at a slightly lingual position. The postmetacristid is short, even shorter than the postprotocristid. It is also transversal to the anteroposterior molar axis and dorso-ventrally oriented. The metaconid is slightly posterior to the protoconid and lower than it. There is a short cristid located at the posterior base of the well-developed and salient metaconid. The talonid is much lower than the trigonid, and the talonid basin is very deep. The hypoconid is partially worn and located at the posteriormost labial portion of the talonid. The cristid obliqua and the postcristid form an angle of less than 90° at the hypoconid. The cristid obliqua is almost parallel to the anteroposterior molar axis. Its anterior border is located just below the protoconid, at the labial end of the postprotocristid. Most of the entoconid is broken, but from its base it can be inferred that it is a large and robust cuspid, antero-posteriorly elongated and labio-lingually compressed. The entocristid is very short. The hypoconulid is well developed, triangular-shaped in occlusal view, and situated posterior and slightly labial to the entoconid. There is a small labial cingulid below the cristid obliqua and a

marked posterior cingulid, running from the hypoconid to almost the labial tip of the hypoconulid. A large posterior root is preserved; the anterior one is broken at its base.

Comments. The following characteristics allowed the assignment of this material to Didelphidae, according to Voss and Jansa (2009): tribosphenic lower molars, with a developed anterior cingulid (notched for the hypoconulid of the preceding tooth), as well as notched paracristids. However, it is important to mention that some authors consider that there are no synapomorphies on the lower molars that undoubtedly characterize the family Didelphidae (Beck *et al*., 2021). Compared to other Miocene didelphids, the TAR-31 specimen is much smaller than *Didelphis solimoensis* Cozzuol, Goin, de los Reyes, and Ranzi, 2006 from Acre (Cozzuol *et al*., 2006), besides having less developed anterior cingulid and more compressed entoconid. Compared to the didelphids from La Venta, Colombia, and according to the measurements reported by Goin (1997) and Suárez Gómez (2019), this material is smaller than the few reported specimens of *Marmosa laventica* Marshall, 1976, and larger than the specimens of *Thylamys minutus* Goin, 1997, but is approximately the same size as *Thylamys colombianus*. *Marmosa laventica* and MUSM 4018 possess a weak cingular shelf present on the labial side between the proto- and hypoconid; in terms of height, protoconid > metaconid > paraconid; trigonid and talonid making up (almost) the same proportion of the crown area; paraconid antero-lingual to protoconid, while the metaconid is slightly posterior to the protoconid (Marshall, 1976). Conversely, MUSM 4018 differs from m1 of *M*. *laventica* in being smaller, in having a protoconid much larger than the paraconid, and a weak development of the anterobasal cingulid (Goin, 1997). Regarding the species of *Thylamys*, MUSM 4018 is larger than the m1s of *T*. *minutus* and does not have a cristid obliqua ending anteriorly below the postprotocristid-postmetacristid notch as in this taxon (Goin, 1997). However, MUSM 4018 is similar to *T*. *colombianus*, in both size and morphology, sharing with this taxon several diagnostic features: comparatively longer and wider talonids; laterally compressed entoconids; less-developed anterior cingulid; paraconid more labially positioned on the trigonid; open preprotocristid not merged with the postparacristid, forming a sharp and open angle with it; preprotocristid oriented approximately along the longitudinal axis of the molar, but not completely parallel to it; cristid obliqua directed towards the protoconid (Goin, 1997; Suárez Gómez, 2019). Nonetheless, MUSM 4018 has a posterior cingulid and a slightly larger paraconid compared to specimens of *T*. *colombianus* described in the literature. According to Suárez Gómez (2019), a paraconid slightly labial to the metaconid is present on the m1 of *T*. *colombianus*

(almost indistinguishable on m2) and a cristid obliqua forming a right angle with the postcristid further occurs on m1 (narrower on m2). Accordingly, we considered MUSM 4018 to be an m1. Based on the described morphology, which mostly fits the diagnostic characters of *T. colombianus*. We left the genus in open nomenclature as '*Thylamys*', since recent phylogenetic studies have considered the genus *Thylamys* to have diverged from other didelphids much later than the age of the deposits of TAR-31 (not until the Pliocene, and, for the last common ancestor of *Thylamys* and *Gracilinanus* + *Cryptonanus*, not until ~10 Ma) (Jansa *et al*., 2014; Beck and Taglioretti, 2020). Thus, it is possible that this taxon and other Miocene allegedly *Thylamys* representatives might not pertain to the *Thylamys* clade, but represent some kind of stem Thylamyini instead.

The presence of a well-developed posterior cingulid in MUSM 4018 is a striking feature, since this structure was until recently considered to be absent in all didelphids, and also in paucituberculatans and microbiotheriids (Beck *et al*., 2021). A posterior cingulid is now described for two didelphids, as well as in basal ameridelphians (Beck *et al*., 2021) and caenolestid paucituberculatans (Abello *et al*., 2021).

MUSM 4018 was previously reported by Antoine as *Marmosa* (*Micoureus*) sp. in Marivaux *et al*. (2020), however, as we argue above, we assign it to '*Thylamys*' cf. '*T.*' *colombianus* instead.

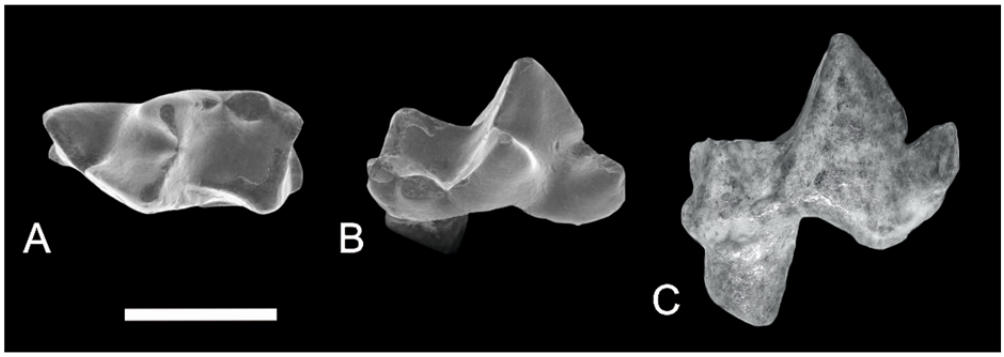

Figure 4. Didelphimorph metatherian from TAR-31, Juan Guerra, San Martín Department, Peru (late middle Miocene). **A**, **B**, and **C**, MUSM 4018, '*Thylamys*' cf. '*T.*' *colombianus*, left m1. **A**, occlusal; **B**, oblique lingual; and **C**, labial views. Scale bar = 1 mm.

Order Paucituberculata Ameghino, 1894

Superfamily Palaeothentoidea Sinclair, 1906

Family Palaeothentidae Sinclair, 1906

Subfamily Palaeothentinae Sinclair, 1906

Genus *Palaeothentes* Ameghino, 1887

aff. *Palaeothentes*

(Figure 5A–F)

Referred material. MUSM 4019, left M1 (Figure 5A–C); MUSM 4020, left broken ?M2 (without paracone, metacone, and stylar shelf); MUSM 4021, right broken m1 (talonid only; Figure 5D–F).

Locality. TAR-31, Juan Guerra, Tarapoto Province, San Martín Department, Peru.

Formation and age. Ipururo Fm., lower member, late middle Miocene (see Marivaux *et al*., 2020).

Measurements. See Table 1.

Description. Upper molars are relatively large and robust. The M1 is subquadrangular in occlusal view. Anteriorly, it has a wide and long anterior cingulum, which extends from a distinct StA, situated on the labial side of the molar, next to the StB, to the cervix, at a point slightly anterior to the preprotocrista mid-portion. The StB is large, high, and situated just in front of the protocone. The posterior crest of StB is long and conspicuous, with first a slightly oblique direction; towards the contact with the StC+D it changes its course, to become ventrally directed. There is a small protuberance on the anterior lingual face of the StB, at almost half its height, that can be interpreted as the reminiscence of the paracone, with its very subtle crests. The protocone has an open L outline in occlusal view. It is wide, low and slightly more protuberant lingually than the metaconule. The postprotocrista is first linguo-labially directed, before to abruptly rotate labially. There is a deep sulcus separating the postprotocrista from the metaconule. At its labial end, there is a well-developed premetaconular cusp. Below this sulcus, on the lingual side of the molar, a marked protuberance is surrounded by an anterior sulcus and a posterior sulcus. The metaconule is situated at the same level of the StC+D, and is large, with pre- and post-metaconular with rounded margins. A well-developed metacone is present on the anterior portion of the StC+D, although being much shorter than the latter. The StC+D is large and subequal to StB in height. The labial side of the M1 is marked by a well-developed cingulum located at the base of the stylar cusps, less developed on the labial side of the StB and mostly noticeable anteriorly and posteriorly to the StC+D and below the ectoflexus, where a small cuspule is present. Although sharing a very similar morphological pattern, MUSM 4020 was identified as a M2 due to its smaller size in comparison with MUSM 4019 (M1), its narrower occlusal proportions and the

presence of a less protruding metaconule. The labial portion of the molar (including stylar cusps) is not preserved, and morphological discrepancies with MUSM 4019 are: shorter anterior cingulum; protocone and metaconule narrower, with a more triangular shape; a more discrete protuberance at the lingual base of the sulcus separating the protocone and metaconule; trigon basin more deeply excavated, with more difference in height between it and the metaconule; and premetaconular cusp less developed. These characters are compatible with the interlocus variation between M1 and M2 of a same taxon.

MUSM 4021 is a broken m1, lacking the trigonid. The talonid is wide and robust. The talonid basin is deep at its central part, but not wide. The metaconid is the highest cuspid preserved. It is conical shaped and has a distinct metaconid posterior crest *sensu* Abello (2013). A long, marked and curved cristid obliqua runs from the hypoconid to the metaconid. The hypoconid is relatively low and triangular shaped. The postentocristid and postcristid are merged, forming a prominent posterior cristid. Below this structure, on the posterior side of the molar, there is a protuberance, the hypoconulid, starting at a central position and continuing to a point below the entoconid, but it is partly broken. The entoconid is wide and just slightly shorter than the metaconid. A well-developed entocristid is obliquely oriented towards the metaconid posterior crest, but it does not contact it.

Comments. According to the diagnostic characters listed by Abello (2007) for Palaeothentidae, the upper molars from TAR-31 can be assigned to this family by possessing metacone located anteriorly to the apex StC+D and a premetaconular cusp. Compared to *Hondathentes cazador* Dumont and Bown, 1997, a low-latitude palaeothentid of uncertain affinities (see Abello, 2007), the TAR-31 taxon differs in that the postprotocrista is not confluent with the hypocone platform (metaconule *sensu* Abello, 2013) on M1, in lacking the metacone on M1-2, in the presence of a premetaconular cusp on M2 (in *Hondathentes* it is absent), and in m1 lacking the entoconid notch (Dumont and Bown, 1997; Abello, 2007). The M1 from TAR-31 has a wide and long anterior cingulum, and the metaconule and StC+D are aligned as in Decastinae; but, in contrast to the latter, it does not have a protocone posterior to the StB (the protocone is labiolingually aligned with the StB in TAR-31 specimen), which is another diagnostic characteristic of decastines. Furthermore, TAR-31 taxon is smaller than all decastine species, and the lower molar possesses a small cristid posterior to the metaconid, which is considered absent in representatives of this subfamily. As of diagnostic features of Palaeothentinae, specimens from TAR-31 also have StB and StC+D aligned transversally to the protocone and metaconule, respectively; in addition, the lower m1 from TAR-31 has a

cristid posterior to the metaconid, as is common among palaeothentines. However, palaeothentines possess a short anterior cingulum on upper molars (Abello, 2007), whereas it is long in MUSM 4019 and MUSM 4020. Accordingly, the TAR-31 palaeothentid has closer affinities with Palaeothentinae.

Among palaeothentines, in *Palaepanorthus* the M1 has a short anterior cingulum and StB larger than StC+D (Abello, 2007); both features are lacking on the M1 from TAR-31. In addition, the TAR-31 taxon differs from *Carlothentes chubutensis* (Ameghino, 1897) in having m1 without cristid obliqua bent in its midline (Abello, 2007). Bown and Fleagle (1993) reported that the species of *Palaeothentes* do not have lower molars with a cristid obliqua bent in its midline, as observed on the m1 from TAR-31. However, since most of the diagnostic features of this *Palaeothentes* are located on lower molars, they cannot be observed on TAR-31 specimens. According to that, we assign the palaeothentinae from TAR-31 to aff. *Palaeothentes*, which is our favored hypothesis, pending the discovery of more material and associated teeth.

Palaeothentes includes nine species: *P. aratae* Ameghino, 1887 (type species), *P. intermedius* Ameghino, 1887, *P. lemoinei* Ameghino, 1887, *P. minutus* Ameghino, 1887, *P. marshalli* Bown and Fleagle, 1993, *P. migueli* Bown and Fleagle, 1993, *P. pascuali* Bown and Fleagle, 1993, *P. relictus* Engelman, Anaya and Croft, 2017, and *P. serratus* Engelman, Anaya and Croft, 2017 (Abello, 2007; Engelman *et al*., 2017). According to Abello (2007), "Among the species of *Palaeothentes* the paracone on M1 is present uniquely on *P. aratae*, *P. marshalli* and *P. migueli*", and, according to Engelman *et al*. (2017), M1-2 of *P. serratus* also have a paracone. As the M1 from TAR-31 displays a very small paracone on the anterior part of the StB, it would be close to the latter species bearing a paracone on M1. However, Engelman *et al*. (2017) also noted the absence of a crestid-like structure posterior to the metaconid on *P. serratus*, differentiating it from the TAR-31 taxon. Concerning other species of *Palaeothentes* bearing a paracone on M1, *P. migueli* is smaller than the TAR-31 taxon, and in addition it displays molars appearing more gracile, with smaller general proportions and more delicate occlusal structures; *P. marshalli* has well-developed paracone and metacone, but upper molars from TAR-31 have an incipient paracone, in addition to be slightly larger than those of *P. marshalli*; and finally, M2s of *P. aratae* do not have a paracone, their anterior cingulum is short, their metacone and premetaconular cusp are small (Bown and Fleagle, 1993; Abello, 2007), and this species is larger than the TAR-31 palaeothentid.

Upper molars from TAR-31 have therefore several palaeothentine features, but the anterior cingulum on M1 is more similar to that observed in Decastinae. The lower molar has

few characteristics preserved because it is broken and lacks its anterior part (trigonid), but seems to be more related to Palaeothentinae than to Decastinae. Among palaeothentines, the TAR-31 taxon appears particularly close to *Palaeothentes*, and more particularly to *P. marshalli* and *P. migueli*, plus *P. aratae* and *P. serratus*, to a lesser extent. However, there are differences between TAR-31 specimens and all the previously described species of *Palaeothentes*. The great taxonomic diversity of *Palaeothentes*, plus the small number of fragments retrieved at TAR-31, in addition to their fragmentary state, hamper a more precise alpha taxonomic assignment for the specimens from TAR-31.

Among palaeothentoids from La Venta, the size of the TAR-31 *Palaeothentes* is consistent with that of the "Palaeothentoidea fam., gen. et sp. indet." mentioned by Suárez Gómez (2019) at La Venta. Nevertheless, the only specimen reported is a dentary with m2, so the comparisons with the molars from TAR-31 are limited. Suárez Gómez (2019) points out that the specimen is morphologically close to those assigned to Palaeothentidae, but it does not possess the diagnostic characteristics of this family. Therefore, it might document a non-palaeothentid palaeothentoid. Since Palaeothentidae features are clearly present on the TAR-31 taxon, most probably the latter does not coincide with this unnamed palaeothentoid taxon from La Venta.

Family Abderitidae Ameghino, 1889

Genus *Pitheculites* Ameghino, 1902

Type species. *Pitheculites minimus* Ameghino, 1902.

Referred species. *Pitheculites rothi* Marshall, 1990 and *Pitheculites chenche* Dumont and Bown, 1997.

Stratigraphical range. Early to late middle Miocene (Colhuehuapian to Laventan SALMAs).

Geographical range. Chubut Province, Argentina (Barranca Sur del Lago Colhué-Huapí locality); Aisén, Chile (Alto Río Cisnes locality); La Venta, Colombia (La Victoria Fm.); Juan Guerra, Peru (locality of TAR-31).

Diagnosis. *Pitheculites* is characterized by the presence of hypertrophied P3 with labial ridges; M1 with wide and long anterior cingulum ending lingually at the occlusal surface, and antero-posteriorly compressed anterolabial root; presence of parastylar cusp on M2; reduced p3 without anterobasal cuspid; antero-posteriorly compressed hypoconids; m2-3 with short cristid obliqua, which has rounded occlusal margins; anterior end of the dentary dorsally projected; molar series obliquely oriented with respect to the antemolar series (Abello, 2007).

***Pitheculites ipururensis* nov. sp.**

(Figure 5G–M)

Holotype. MUSM 4024, right m2 (Figure 5I–J).

Referred specimens. MUSM 4022, right broken m1 (Figure 5G–H); MUSM 4023, left broken m1 (Figure 5K–M).

Etymology. The specific name, *ipururensis*, derives from Ipururo Fm., which crops out at TAR-31.

Type locality. TAR-31, Juan Guerra, Tarapoto Province, San Martín Department, Peru.

Type formation and age. Ipururo Fm., lower member, late middle Miocene (see Marivaux *et al*., 2020).

Measurements. See Table 1.

Diagnosis. *Pitheculites* of intermediate size, being closer to the size of *P. rothi*. It differs from other representatives of *Pitheculites* in having longer cristid posterior to the metaconid and a wider hypoconulid shelf on the m2. It differs from *P. rothi* in having a narrower and less quadrangular m2, with short and narrow trigonid, paraconid present (as in *P. minimus*), postentocristid more posteriorly positioned and merged with the postcristid, and postcristid oblique. It differs from *P. chenche* in having a crestid-like postentocristid in m1. It differs from *P. minimus* in having m1 with a cuspid-like entocristid (as in *P. chenche*), while in *P. minimus* it is crested-like.

Description. Both m1s are broken in front of the metaconid. Despite that, the typical plagiaulacoid m1 of Abderitidae can be recognized, with a blade-like trigonid, small and basined talonid, and considerable crown height. The lateral cristids and denticles normally present on this locus are not preserved, and MUSM 4022 is slightly larger and higher than MUSM 4023. The labial side of the preserved trigonid portion is labiolingually compressed, making the trigonid much narrower than the talonid at this point. Both specimens preserve a small posterior protuberance on the occlusal surface of the shearing blade, that according to Abello (2013: figures 4DA, D-E), is homologous to the metaconid, which is joined to the anterior extremity of a long vertical cristid obliqua. On the less-worn MUSM 4021, the cristid obliqua is composed of one anterior long, vertical labially-oriented segment, followed by a small, lingually-oriented one, both forming an angle of ~90°. On the other hand, both segments are completely merged, forming one long, curved labial cristid on MUSM 4022.

The entoconid is small and it has a short and cuspid-like entocristid; the postentocristid is joined with the postcristid forming a complete cristid. The hypoconid is located at the posteriormost portion of the talonid, forming an angle of almost 90° with the postcristid. A small hypoconulid is visible posterior to and below the postcristid.

The m2 has a rectangular shape and it is wider than the m1 at its base. The trigonid is narrower and much shorter than the talonid. The labial margin is higher than the lingual one. There is a well-developed anterolabial trigonid cusp *sensu* Abello (2013: fig 4B), positioned anterior to the protoconid and much higher and larger than the paraconid. Between the trigonid anterior cuspid and the paraconid and metaconid there is a deep narrow basin. A well-developed hypoconulid notch is present just below the anterolabial trigonid cuspid. The paraconid is not very well developed, restricted to a small triangular protuberance at the base of the premetacristid, slightly labial to the metaconid. The metaconid is well developed, but smaller and shorter than the protoconid, being much more anteriorly positioned than the latter. There is a short postmetacristid, and a distinct metaconid posterior crest *sensu* Abello (2013) is present, lingual and posterior to the metaconid, directed towards the entocristid. The protoconid is the largest and tallest cuspid of the molar. The protocristid is incipient, being visible almost only at its base. A well-developed and protuberant protoconid posterior crest *sensu* Abello and Rubilar-Rogers (2012) is present, posterior and labial to the protoconid. At the posterior extremity of this protoconid posterior crest, a deeply excavated sulcus separates it from the cristid obliqua, and the posterior wall of this sulcus is S-shaped. The cristid obliqua is very short and almost sagittal. Besides, it has a rounded occlusal outline and a deep circular excavation at its lingual side. The hypoconid is small and antero-posteriorly compressed, located slightly posterior to the entoconid. A well-marked postcristid is present; it is oblique, connecting to the postentocristid posteriorly to the midline of the teeth. The postentocristid is very well developed, posterolabially directed, forming a small cuspid at the posterolingual extremity of the molar. This cuspid formed by the postentocristid is separated from the entoconid by a deep sulcus. Below the postcristid and postentocristid, a pronounced hypoconulid forms a posterior and ventral shelf covering most of the molar posterior surface. The entoconid is high and wide at its base. Anterior to the entoconid, a very well-developed entocristid forms a well-defined cuspid. The latter is separated from the metaconid by the conspicuous metaconid posterior crest. The postentocristid plus the entoconid and the entocristid form a set of three marked cuspids on the lingual side of the talonid. The talonid basin is deep, but narrow, due to the widening of the basal portion of the talonid cuspids.

Comments. The assignment of these specimens to Abderitidae is based on the following characters: presence of anterolabial cuspid on the trigonid of m2, and protocristid notch not developed on m2 (Abello, 2007). Among abderitid genera, these remains can be referred to *Pitheculites* by having a small and anteroposteriorly-compressed hypoconid and a short cristid obliqua with rounded occlusal margin on m2 (Abello, 2007). Three species of *Pitheculites* are currently recognized: *P. minimus* Ameghino, 1902, *P. rothi* Marshall, 1990, and *P. chenche* Dumont and Bown, 1997. *Pitheculites ipururensis* nov. sp. from TAR-31 is slightly larger than *P. minimus*, with narrower m2, but, as this species, it has a paraconid on m2, and the postentocristid of m1 is sharp (not rounded as in *P. chenche*). *Pitheculites ipururensis* nov. sp. differs from *P. rothi* in having a much shorter trigonid on m2, the postcristid not merged with the entoconid, but with the postentocristid, and a postcristid less transversally oriented (in *P. rothi* the postcristid is more transversally oriented on m2, and rather oblique on m3). The unique specimen of *P. chenche*, a partial right dentary preserving p3–m3 (IGM 250941), has much worn teeth. Nevertheless *P. ipururensis* nov. sp. is clearly smaller and it has sharp postentocristid on m1. The m2 of *P. ipururensis* nov. sp. is also less quadrangular than in *P. chenche,* with a labiolingually narrower trigonid, a longer cristid posterior to the metaconid, a more posterior postentocristid, and a wider hypoconulid shelf.

Concerning body mass, according to the equation of Dumont *et al*. (2000), but adding the SE (see Abello *et al*., 2020, SM5):

$$x = \text{m2 area};\ \log y = 2.419 + 1.727\ (\log x);\ SE = 1.16$$

the body mass of *P. ipururensis* nov. sp. is estimated at 44.62 g, while that of *P. chenche* is at 108.67 g, *P. rothi* 61.45 g, and *P. minimus* 35.82 g.

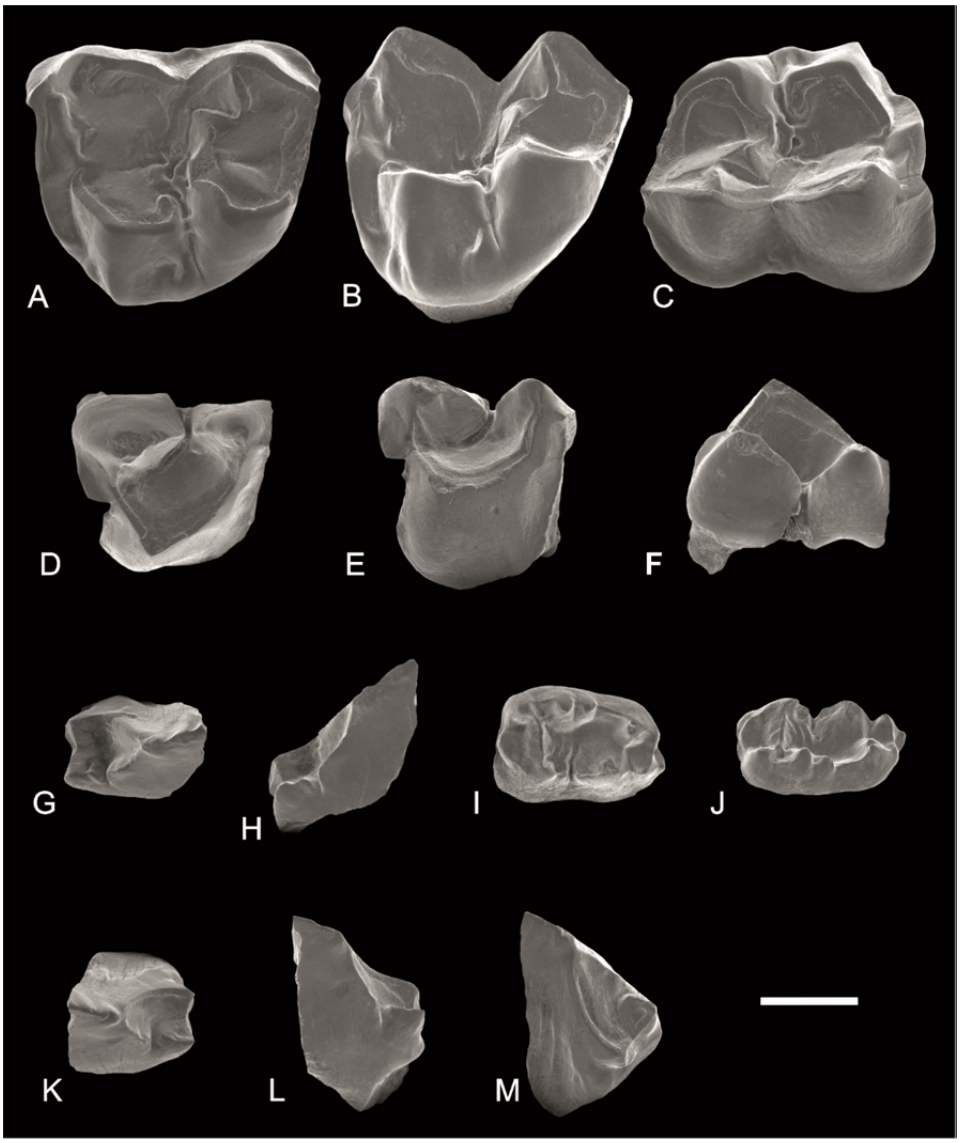

Figure 5. Paucituberculatan metatherians from TAR-31, Juan Guerra, San Martín Department, Peru (late middle Miocene). **A**–**F**, aff. *Palaeothentes*, **A**–**C**, MUSM 4019, left M1; **D**–**F**, MUSM 4021, right m1. **G**–**M**, *Pitheculites ipururensis* nov. sp., **G**–**H**, MUSM 4022, left m1; **I**–**J**, MUSM 4024, right m2 (**holotype**); **K**–**M**, MUSM 4023, right m1. **A**, **D**, **G**, **I**, and **K**, occlusal; **B**, **E**, **H**, **J**, and **L**, lingual; and **C**, **F**, and **M**, partially labial views. Scale bar = 1 mm.

Table 1. Dental measurements (in mm) of molars of '*Thylamys*' cf. '*T.*' *colombianus* (Didelphimorphia), aff. *Palaeothentes*, and *Pitheculites ipururensis* nov. sp. (Paucituberculata) from TAR-31, Juan Guerra, San Martin Department, Peruvian Amazonia (late middle Miocene).

Taxon	Specimen	Length	Width
'*Thylamys*' cf. '*T.*' *colombianus*	MUSM 4018 (m1)	1.73	0.89
aff. *Palaeothentes*	MUSM 4019 (M1)	3.07	2.77
	MUSM 4020 (broken ?M2)	2.76	1.92
	MUSM 4021 (m1, talonid only)	2.10	1.88
Pitheculites ipururensis sp. nov.	MUSM 4022 (broken m1)	Total = 1.83 Talonid = 1.17	Trigonid = 1.33 Talonid = 1.18
	MUSM 4023 (broken m1)	Total = 1.85 Talonid = 1.16	Trigonid = 1.02 Talonid = 1.09
	MUSM 4024 (**holotype**, m2)	Total = 1.80 Trigonid = 0.66 Talonid = 1.13	Trigonid = 1.15 Talonid = 1.29

5. Discussion and Conclusions

5.1 Taxonomy, paleobiology and paleoecology of the metatherians from TAR-31

Despite the low number of fossil specimens (only seven teeth or tooth fragments) and the limited extension of the outcrop (5 m^2, *i.e.*, strongly contrasting with La Venta), the metatherian assemblage recorded at TAR-31 can be considered fairly diverse with three taxa belonging to three distinct families and two orders. It can be hypothesized that more marsupial taxa could have been recovered through a wider sampling effort (Magurran, 2004), but the fossil-yielding lens has been fully analyzed in TAR-31 (Marivaux *et al.*, 2020).

Thylamys, probably represented at TAR-31 by '*T.*' cf. '*T.*' *colombianus*, is a genus recovered as monophyletic in recent phylogenetic analyses, which typifies the Thylamyini, and includes at least nine small-sized living species (Voss and Jansa, 2009). As reported by Suárez Gómez (2019), the estimated body mass of *T. colombianus* is approximately 52 g, being larger than *T. minutus* (~13 g), also reported at La Venta. Suárez Gómez (2019) additionally suggested that, according to its dental morphology, *T. colombianus* would have had insectivorous/faunivorous habits.

As to the paucituberculatans from TAR-31, *Palaeothentes* was recently recovered as a monophyletic genus, when *Palaepanorthus* (*Palaeothentes*) *primus* is excluded (Abello, 2013; Engelman *et al*., 2017). Nevertheless, the species with which aff. *Palaeothentes* from TAR-31 seems to have stronger affinities, *i.e*., *P. aratae*, *P. marshalli*, *P. migueli*, and *P. serratus*, are not closely related in that same phylogeny (Engelman *et al*., 2017; see also Abello *et al*., 2020), the retention of the paracone seeming to be a plesiomorphic trait. Based on the protocol proposed by Dumont *et al*. (2000), only *P. serratus* is hypothesized to have been insectivorous, whereas all three other species were unambiguously interpreted as frugivorous (Engelman *et al*., 2017). Unfortunately, because no m2 has been recovered for aff. *Palaeothentes* at TAR-31 it is not possible to perform a dietary reconstruction for this taxon. The aff. *Palaeothentes* from TAR-31 had an intermediate size, far from larger species of palaeothentids, such as *P. aratae* and *Titanothentes simpsoni* Rae, Bown, and Fleagle 1996, with an estimated weight over 500 g, and larger than the small species of the genus (*e.g*., *P. marshalli* and *P. migueli*, with less than 250 g; Abello *et al*., 2020: SM5). In fact, when compared with the coeval species of *Palaeothentes* from Quebrada Honda, aff. *Palaeothentes* from TAR-31 is larger than *P. serratus*, which has estimated body mass of approximately 100 g, being closer in size to that of *P. relictus*, estimated to have weighted around 150 g (Engelman *et al*., 2017). Palaeothentids were particularly diverse in high-latitude early Miocene localities, with, for instance, six species reported in the Santa Cruz Fm. (Abello and Candela, 2010), plus four other ones in the Pinturas Fm. (Abello, 2007), with body masses ranging from 44 g to 980 g. Some authors suggest that they were abundant in somewhat dry and open habitats, with mixed vegetational cover and seasonal aridity (Engelman *et al*., 2017). Nevertheless, they still favored habitats with relatively high rainfall, explaining their diversity in the Santa Cruz and Pinturas formations, which were not particularly dry (Kramarz and Bellosi, 2005; Spradley *et al*., 2019). Furthermore, the abundance of palaeothentids in lower Oligocene layers of the Shapaja section, located few km away from TAR-31, presumably supports this hypothesis, since this region went through a drier period by the Eocene–Oligocene transition (Antoine *et al*., 2021; Stutz *et al*., 2021).

Among Abderitidae, *Pitheculites* is closely related to *Abderites*, a genus spanning the early–middle Miocene interval in Argentina and Chile (Abello and Rubilar-Rogers, 2012). Both genera are more distantly related to *Parabderites*, which has a more plesiomorphic morphology and is recorded in the Oligocene–early Miocene of central Patagonia and Chile (Abello, 2007, 2013). The representatives of *Pitheculites* are among the smallest non-pichipilid palaeothentoids (with a body mass ranging from ~30 to 100 g), differing from

representatives of *Abderites* (~280–600 g; Abello *et al*., 2020: SM5). Abderitid dental morphology is interpreted as having allowed the consumption of a wide array of food items, even those with hard covers, making them dietary generalists (Dumont *et al*., 2000). Abderitids would have been more frugivorous than palaeothentids, and a positive correlation between high precipitation rates and the abundance of fruit/frugivores has been recorded (Kay and Madden, 1997). In contrast with palaeothentids, the great abundance of abderitids seems to be a signature of forested areas under wet humid climates, where there would be more fruit and frugivores (Engelman *et al*., 2017).

When detailing the preliminary identifications of the marsupial fauna of TAR-31, Marivaux *et al*. (2020) mentioned the occurrence of "an argyrolagid marsupial" based on a fragmentary high-crowned molar. According to our current evidence, we cannot confirm this assignment, as the tooth in question likely pertains to a pristine deciduous molar of a tiny hegetotheriid instead. Despite not being present in TAR-31, argyrolagids have already been identified in Peruvian Amazonia: one tooth of an indeterminate taxon, being reported from the lowermost late Miocene levels near Contamana (CTA-43 locality, Pebas Fm.; Antoine *et al*., 2016), and dozens of isolated teeth recovered in various latest Eocene–early Oligocene vertebrate assemblages from the Shapaja section, San Martín (*Proargyrolagus* spp.; Antoine *et al*., 2021), thereby suggesting a long-lasting presence for this singular and elusive family in Western Amazonia.

Strikingly, flesh-eating Sparassodonta are not recorded at TAR-31, whereas they are often present in Miocene deposits at mid- and low latitudes of South America, with great diversity. In particular, sparassodonts are remarkably diverse at La Venta, In Colombia, with four species of at least three families already described (Hathliacynidae, Hondadelphidae, and Thylacosmilidae; Suárez Gómez, 2019). In addition to the taxa from La Venta, one taxon is reported for the Castilletes Formation in Colombia (the sparassodontan *Lycopsis padillai*, Suárez *et al*., 2016); in Bolivia, three taxa of at least one family in Quebrada Honda (Hathliacynidae; Engelman *et al*., 2020), one taxon in Cerdas (a new Borhyaenoidea still to be described, Croft *et al*., 2016), and Achiri (*Borhyaenidium altiplanicum*, Villarroel and Marshal, 1983) in Bolivia; one possible taxon in Urumaco, Venezuela (Linares, 2004); and a hathliacynid at Madre de Dios (MD-67 locality; Antoine *et al*., 2013), a premolar of uncertain affinities at CTA-44 (Contamana, earliest late Miocene, Pebas Fm.; Antoine *et al*., 2016), and one possible record at the Fitzcarrald local fauna (Tejada-Lara *et al*., 2015) in Peru. This absence could be due to specific taphonomic biases (*i.e*., size sorting), such as the small size of sediment grains and fossil specimens trapped in TAR-31, thus not favoring the preservation

of large-sized fossil taxa, and that sparassodonts are generally rare in South American fossil faunas. Meso- and macrovertebrates are scarce at TAR-31 and documented only by few fragments of teeth (not complete specimens). Ecological reasons (*e.g.*, low ecomorphological disparity) may further explain this unbalanced metatherian sample (see Croft *et al.*, 2018).

Microbiotheria are absent from TAR-31, but also from Quebrada Honda and other Miocene localities at low latitudes (Goin, 1997; Suárez Gómez, 2019). The single known record from La Venta is the northernmost occurrence of the order. The origin, radiation and dispersal of microbiotheres are thought to have occurred in the Austral Kingdom, *i.e.*, southernmost South America and Antarctica (Goin *et al.*, 2016). They are especially recorded in lower Miocene deposits of Patagonian Argentina, a period and an area where they should have reached their peak diversity (Chornogubsky and Kramarz, 2012; Goin and Abello, 2013; Goin *et al.*, 2016), being also recorded in the Antarctica Peninsula (Goin *et al.*, 1999). Microbiotherian diversity remained low and stable throughout the entire Paleogene, and they are represented today by a sole taxon, *Dromiciops*, with very limited distribution in southern South America (Quintero-Galvis *et al.*, 2021).

In addition, among micromammals, it is also worth noting the low metatherian *vs*. rodent remains ratio at TAR-31 (0.018), with ~400 rodent specimens and seven metatherian remains. However, in terms of taxonomic richness, the discrepancies between rodent and metatherian assemblages are not as extensive, since despite the small sample size, three different metatherians belonging to two superfamilies are so far documented at TAR-31, whereas rodents are represented by nine taxa pertaining to four superfamilies (Boivin *et al.*, 2021). In general, it should be added that fossil remains of rodents are considerably more abundant than metatherian specimens in the Eocene–Miocene vertebrate localities of Western Amazonia, being the most species-rich mammalian group in Santa Rosa, Contamana (Pozo, Chambira, and Pebas formations) and the Shapaja section, for example (Frailey and Campbell, 2004; Antoine *et al.*, 2016, 2021; Boivin *et al.*, 2017a, b, 2018; Arnal *et al.*, 2020, 2022). The causes of this disparity remain to be better explored. There might be taphonomic biases, such as sampling biases, predator preference towards specific prey, prey's abundance and preferred habitats, affecting the taxa abundance and richness in the available samples. Nevertheless, this unbalanced pattern could also be related to the consequences of the climatic and environmental shift triggered around the Eocene–Oligocene transition, with drastic impacts recorded on metatherian faunas, at least in the Southern cone of South America (Goin *et al.*, 2010, 2016), impacts remaining to be better assessed at low latitudes (Antoine *et al.*, 2021).

5.2 Biostratigraphical and chronostratigraphical implications

The age of the TAR-31 fossil assemblage has been proposed to be ranging from 13.1 to 12.5 Ma, as inferred through mammalian biostratigraphy (Figure 2) (Marivaux *et al.*, 2020; Boivin *et al*., 2021). Two metatherian taxa documented here are similar to species recovered at the La Venta deposits thus far, which do not have overlapping stratigraphic ranges (‘*Thylamys*’ cf. ‘*T.*’ *colombianus* at *ca*. 13.0 Ma and *Pitheculites chenche* at *ca*. 13.5 Ma), according to the magnetostratigraphical age estimates of Madden *et al.* (1997), as revised by Raffi *et al*. (2020). However, these small discrepancies are most likely due to sampling biases with such a poor record, as very few localities were screen-washed at La Venta (Madden *et al*., 1997).

Recently, Castro *et al*. (2021), when revising the fossil record of Didelphidae from South America, considered that the middle Miocene didelphids from Madre de Dios (MD-67), La Venta, and now also TAR-31, could be considered one of the first reliable occurrences of crown representatives of the family, along with the records presented by Goin *et al*. (2007) for Argentine Patagonia. The records of two species of *Thylamys* in La Venta (*ca*. 13.0 Ma; see above) are the earliest occurrences for the genus, and the recognition of ‘*T.*’ cf. ‘*T.*’ *colombianus* at TAR-31 substantiates this statement as a result (13.1–12.5 Ma, and more probably 13.1–13.0 Ma; Marivaux *et al.*, 2020; Boivin *et al.*, 2021). Conversely, the record of *Pitheculites ipururensis* nov. sp. from TAR-31 (13.1–12.5 Ma) might slightly postdate the former last appearance of Abderitidae, previously documented by *P. chenche* in La Venta (*ca*. 13.5 Ma; see above). Following the Oligocene radiation of palaeothentoids, the early–early middle Miocene is considered as the climax of paucituberculatans’ evolutionary history, with a high taxonomic diversity of abderitids and palaeothentids (Abello *et al*., 2020). After Laventan times, Palaeothentoidea became extinct and only the Caenolestoidea have persisted until today among paucituberculatans (Engelman *et al*., 2017; Abello *et al*., 2021). Surprisingly, palaeothentoids were still very diverse and abundant in several Laventan localities *i.e*., La Venta, Quebrada Honda and now TAR-31, suggesting that their extinction did not occur as a long decline, and more like an abrupt event triggered by reasons still poorly understood (Engelman *et al*., 2017). Nevertheless, the early late Miocene interval is particularly underrepresented (and perhaps under-sampled) at low latitudes and especially in Western Amazonia (Antoine *et al.*, 2017), which prevents further discussion on this issue at the time being.

The calculated MDA of 17.4 ± 0.12 Ma is ~4 My older than the biostratigraphical age of the sample. Hence, we interpret this MDA as a detrital provenance age. This temporal hiatus might be related to the low volcanic activity during late early and early Miocene times upstream in the corresponding drainage basin, contrary to what occurs in the adjacent Bagua Basin (Moreno *et al*., 2020). Potential source for these early Miocene zircons may include the Callipuy volcanic arc located in the Peruvian Western Cordillera (Navarro *et al*., 2010) or the Saraguro Fm. located in the Inter-Andean region of Southern Ecuador (see Hungerbühler *et al*., 2002 and references therein).

Overall, we interpret TAR-31 to be mainly sourced by Andean terrains, because 25.3% of the analyzed zircons are younger than 500 Ma and hence derived from Andean magmatic rocks (see Hurtado *et al*., 2018 and references therein). Older Meso-Proterozoic zircon grains related to the Amazon Craton provinces of Rio Negro-Jurena (1.82–1.54 Ga), Rondonia San Ignacio (2.0–1.82 Ga), and Greenville Sunsás (1.3–0.9 Ga) and to the Brazilian Neoproterozoic mobile belts (0.7–0.5 Ga), are interpreted as reworked ancient sedimentary rocks, likely Cretaceous sedimentary rocks that are cratonic in provenance (Erlich *et al*., 2018; Hurtado *et al*., 2018; Louterbach *et al*., 2018). However, despite the large number of older grains, the presence of younger zircons grains strongly suggests an Andean orogenic source during the early middle Miocene that conditioned the provenance and filling of this part of the Huallaga basin at that time, at the western edge of the PMWS.

The Cretaceous Andean Arc zircon age population could be sourced by granites of the Coastal Batholith (100–50 Ma) located in the Western Cordillera (Litty *et al*., 2017). The Permo-Triassic zircon grains could be sourced by the acid volcanics of the Lavasen Fm. (Upper Paleozoic) and the Triassic Rift Mitu (Lower Mesozoic), which were preserved in the northern part of the Eastern Cordillera (Eude *et al*., 2015). Those sequences were affected by an eastward propagation of the Eastern Cordillera (Eude *et al*., 2015), which could be exposed and eroded at that time. However, despite the Miocene uplift of the Eastern Cordillera (Eude *et al*., 2015), we suspect that the Eastern Cordillera was not high enough to act as a topographic barrier because of the presence of the potential zircons from Callipuy volcanic arc (Western Cordillera; Navarro *et al*., 2010) and from Saraguro Fm. (Inter-Andean; Hungerbühler *et al*., 2002) and of the lowest elevation of Eastern Cordillera around 17.6 Ma (Eude *et al*., 2015).

5.3 Paleoenvironmental inferences

The presence of abderitids, along with a cebid primate at TAR-31, suggests predominantly humid and warm tropical conditions, with the occurrence of surrounding forests (Marivaux *et al.*, 2020; see subsection 5.1). Taxonomy, paleobiology and paleoecology of the marsupials from TAR-31). Palaeothentids seemingly preferred drier habitats, but still relatively humid, with mixed vegetational cover (Engelman *et al*., 2017), which would point, to some extent, to a landscape heterogeneity in the concerned area at that time. Aquatic faunal components retrieved at TAR-31 are primarily related to freshwater environments (ichthyofauna, turtles, caimans and gharials, and decapods; Marivaux *et al*., 2020). However, isotopic analyses made on crab claws and fish teeth from TAR-31 (Alvim *et al*., 2021) point to potential oligohaline conditions, suggesting marine influence, consistent with the hypothesized landscapes as reconstructed at the western margin of the Pebas Mega-Wetland System (Hoorn *et al.*, 2010; Roddaz *et al.*, 2010; Boonstra *et al.*, 2015; Antoine et al., 2016; Marivaux *et al.*, 2020; Alvim *et al*., 2021).

5.4 Paleobiogeographical implications

The Amazonian region has been regarded as a key area concerning the Neogene marsupial radiations (Goin, 1997; Antoine *et al*., 2017; Suárez Gómez, 2019; Castro *et al*., 2021). The records from La Venta, for instance, suggest that this area was both a "cradle", *i.e*., a high-diversification rate area, as well as a "museum", with low extinction rates (Suárez Gómez, 2019).

All three marsupial genera recognized at TAR-31 have broad temporal and geographical ranges. *Thylamys* has extant representatives inhabiting subtropical South America, with records from Peru southwards along the Andes and Chilean Pacific coast, as well as eastwards across Argentina, Bolivia, Brazil, Paraguay, and Uruguay, inhabiting almost exclusively arid to semiarid environments and being especially diverse in the region between the Altiplano and northern Patagonia (Gardner, 2007; Voss and Jansa, 2009). Other species of *Thylamys*, either extinct or extant, neither occur in Amazonia nor in the lowermost latitudes. Accordingly, the La Venta and TAR-31 records suggest a distinct and much broader past geographical range for this genus. Besides, other fossil species of *Thylamys* are recorded in the late Miocene of the Pampean Argentina (Buenos Aires and La Pampa provinces, *T. pinei* Goin, Montalvo and Visconti, 2000 and *T. zetti* Goin, 1997; Huayquerian SALMA; Goin, 1997; Goin *et al*., 2000; Verzi *et al*., 2008), as well as in lower Pliocene deposits of the Buenos Aires Province (*T. contrerasi*; Montehermosan SALMA; Goin, 1997; Prevosti *et al*.,

2021), and Pleistocene/Holocene localities of Argentina and Brazil (Deschamps and Tonni, 1992; Hadler *et al*., 2009; Motta *et al*., 2019). However, as mentioned above, further analyses are needed to confirm if these Miocene *Thylamys* representatives indeed pertain to *Thylamys sensu stricto* or to some kind of stem Thylamyini instead.

Palaeothentes is a speciose genus with several species recorded in early and middle Miocene deposits of Argentina and Chile (Río Frías Fm., Chile; Sarmiento, Santa Cruz, and Pinturas formations, Argentina; Colhuehuapian to Friasian SALMAs; Abello, 2007), as well as in Quebrada Honda, Bolivia (Honda Group, late middle Miocene; Engelman *et al*., 2017). Aside from *Pitheculites ipururensis* nov. sp., *Pitheculites* includes the early Miocene *P. minimus* from Argentinean Patagonia (Sarmiento Fm., Colhuehuapian SALMA), the early middle Miocene *P. rothi* from Chile (Río Frías Fm., "Friasian" age), and the late middle Miocene *P. chenche* from La Venta, Colombia (Honda Group, La Victoria Fm., Duke 113 locality; *ca*. 13.5 Ma) (Abello, 2007). *Pitheculites* stands out among abderitids due to its remarkably broad temporal and geographical distribution, spanning around 8 My (21–13.0 Ma) and 50° in terms of latitude, with records from Patagonian Argentina (*ca.* 45°S; the oldest and southernmost ones) to equatorial Colombia (*ca.* 5°N; Abello, 2007) and Peruvian Amazonia (TAR-31; *ca*. 13.0 Ma, 6°30'S). The general pattern is that of a northern shift or northward contraction of the distribution range, strikingly recalling that of astrapotheres and South American monkeys, in the very same time interval (Fleagle *et al*., 1997; Hartwig and Meldrum, 2002; Goillot *et al.*, 2011; Rosenberger and Hartwig, 2013; Kay, 2015; Marivaux *et al*., 2016a, b, 2020).

The palaeothentoid record in Western Amazonia has been widely expanded in the two last decades, through the middle Eocene–Miocene assemblages from Contamana (Pozo, Chambira, and Pebas formations; Antoine *et al*., 2016), the mid-Paleogene Santa Rosa fauna (Goin and Candela, 2004), the upper Eocene–lower Oligocene Shapaja section (Pozo Fm.; Antoine *et al.*, 2021), and the late middle Miocene La Venta fauna (Suárez Gómez, 2019). This long and diverse presence of palaeothentoids in northern South America may represent a key chapter of their evolutionary history, which remains open.

Comparisons with other Miocene metatherian assemblages at low and mid latitudes of South America find that TAR-31 shows the closest relationship to La Venta, as was already noticed for other mammalian groups (Marivaux *et al.*, 2020; Boivin *et al.*, 2021). In general, TAR-31 shows still closer affinities with the mammalian assemblage from the lower part of the Villavieja Fm. at La Venta (13.1–12.5 Ma; Madden *et al.*, 1997), in sharing a cebid primate (*Neosaimiri*; Marivaux *et al*., 2020), three rodent species (Boivin *et al*., 2021), the

medium-sized notoungulate *Miocochilius*, and the proterotheriid litoptern *Megadolodus* (Marivaux *et al*., 2020; Boivin *et al*., 2021). This strong similarity is further supported by metatherians, as all three families of marsupials recorded at TAR-31 (Didelphidae, Abderitidae, and Palaeothentidae) are also documented at La Venta, with one species (‘*Thylamys*’ cf. ‘*T.*’ *colombianus*) and one genus (*Pitheculites*) in common, despite the fact that the latter comes from a single level of the slightly older La Victoria Fm. (Goin, 1997; Madden *et al*., 1997; Suárez Gómez, 2019). The La Venta fauna contains two additional metatherian orders (Sparassodonta and Microbiotheria) and five extra families (Hondadelphidae, Hathliacynidae, Thylacosmilidae, ?Sternbergiidae, and Microbiotheriidae; Suárez Gómez, 2019), which are not recorded at TAR-31. The localities of Madre de Dios (MD-67; Antoine *et al.*, 2013) and Acre in Brazil and Peru (Río Acre, Czaplewski, 1996; Cozzuol *et al*., 2006) also have close affinities with TAR-31 by recording didelphids as well. The other species-rich metatherian assemblage from the Laventan SALMA is Quebrada Honda (13.1–12.4 Ma; Gibert *et al*., 2020), which is mostly distinct from TAR-31, by sharing one single taxon (*Palaeothentes*, family Palaeothentidae). Abderitids and didelphids, occurring at TAR-31, are not recorded in Quebrada Honda. Conversely, sparassodonts are species-rich, but fairly rare, at Quebrada Honda and absent from TAR-31. Argyrolagid polydolopimorphians and decastine palaeothentids are also present in Quebrada Honda deposits and absent at TAR-31 (Engelman *et al*., 2015, 2017, 2020). Therefore, these similarities between the metatherian fauna from TAR-31 and the ones from mid and high latitudes of South America further support the hypothesis that Western Amazonia represented a single and consistent biogeographical region for land mammals over middle Miocene times, probably due to the region's strong relationship within the PMWS (Figure 6). On low latitudes of South America, during the Miocene (from ~16,5 Ma), the orogeny of the Andes started to have a great influence on the climate, by preventing humid air from the southern Pacific to reach eastern forelands, leading to an increase in aridity and cooler temperatures, and thus to the disappearance of tropical and subtropical climates in the southern part of the continent (Blisniuk *et al*., 2005). Until today, the Andean Cordillera is considered a major factor disrupting atmospheric circulation, generating several local and also broad phenomena, such as differences between climatic conditions on its eastern and western slopes and adjacent areas (Garreaud, 2009).

In the present contribution we have described the records of ‘*Thylamys*’ cf. ‘*T.*’ *colombianus*, aff. *Palaeothentes* and *Pitheculites ipururensis* nov. sp. for the late middle Miocene locality of TAR-31, Peruvian Amazonia. These records expand our knowledge of

the metatherian diversity during the Miocene in Western Amazonia, partly fulfilling the gap in the knowledge of fossil metatherians from northern South America. Additionally, the data presented here strengthen the idea that Western Amazonia formed a significant unit in terms of paleobiogeography under the influence of the PMWS during middle Miocene.

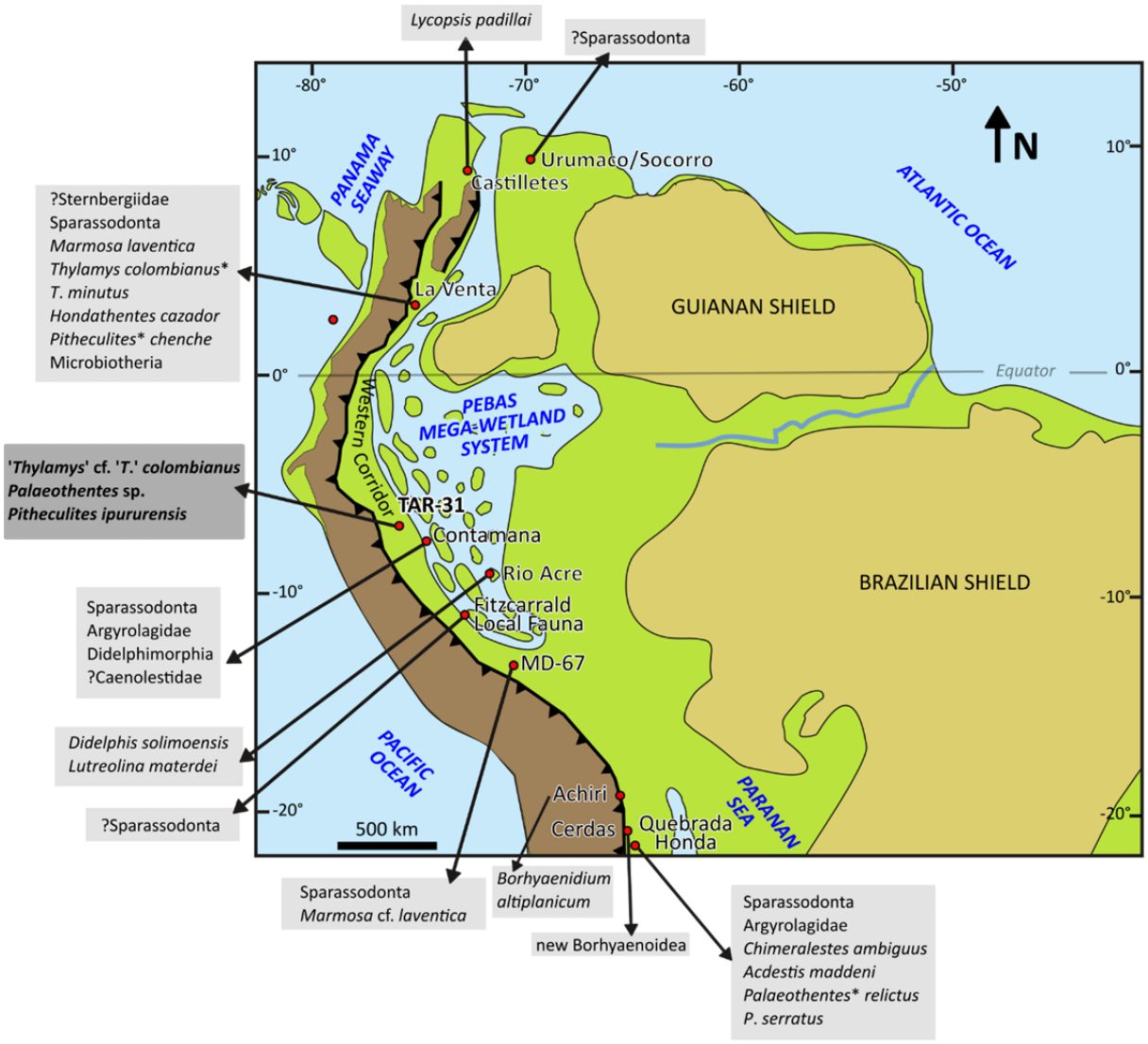

Figure 6. Late middle Miocene (*ca*. 13 Ma) paleogeographic map of Northern South America with the Metatheria taxa recorded in each one of the fossiliferous localities mentioned in the text (red dots). Light green shows low-elevation terra firma forests. Shape and size of emerged landmasses within the Pebas Mega-Wetland System (PMWS) are tentative. Modified from Hoorn *et al*. (2010), Antoine *et al*. (2013), Boonstra *et al*. (2015), Anderson *et al*. (2016), and Marivaux *et al*. (2020). Paleoecological data from Croft (2007), Cadena *et al*. (2015), Tejada-Lara *et al*. (2015), and Antoine *et al*. (2016, 2017). Faunal lists according to Villarroel and Marshal (1983), Czaplewski (1996), Linares (2004), Cozzuol *et al*. (2006), Antoine *et al*. (2013, 2016), Tejada-Lara *et al*. (2015), Croft *et al*. (2016), Suárez *et al.* (2016), Engelman *et al*. (2017, 2020), and Suárez Gómez (2019). * indicates taxa in common with TAR-31.

Acknowledgments

We thank all the people who participated during the fieldwork campaigns and C. Cazeveille (INM, France) for the access to the SEM facilities. We are highly indebted to Russell K. Engelman and an anonymous reviewer for their constructive and in-depth comments of a former version of this manuscript. This work was supported *by Conselho Nacional de Desenvolvimento Científico e Tecnológico* (CNPq, 140773/2019-3, 312941/2018-8, 306951/2017-7), *Coordenação de Aperfeiçoamento de Pessoal de Nível Superior* (CAPES, COFECUB program Te 924/18 "Paléo-Amazone: evolution Néogène de l'Amazonie Brésilienne", 88881.143095/2017-01), the National Geographic Society (nº 9679-15), the Campus France program of the French Ministry of Foreign Affairs, the *Institut des Sciences de l'Évolution de Montpellier* (ISEM), The Leakey Foundation, the French *Agence Nationale de la Recherche* ("*Investissements d'Avenir*" grant LabEx CEBA, ANR-10-LABX-25-01), and the international programs of cooperation ECOS-FonCyT (A14- U01), and CoopIntEER CNRS-CONICET (nº 252540). The paleontological investigations in Peru occur in the framework of the cooperation agreement between the ISEM and MUSM. This is ISEM publication n°: 2022-149 SUD.

References

Abello, M.A. 2007. Sistemática y Bioestratigrafía de los Paucituberculata (Mammalia, Marsupialia) del Cenozoico de América del Sur. Ph.D. Thesis (Unpublished), Universidad Nacional de La Plata: 381 p.

Abello, M.A. 2013. Analysis of dental homologies and phylogeny of Paucituberculata (Mammalia: Marsupialia). Biological Journal of the Linnean Society 109(2): 441–465. doi:10.1111/bij.12048

Abello, M.A.; Candela, A.M. 2010. Postcranial skeleton of the Miocene marsupial *Palaeothentes* (Paucituberculata, Palaeothentidae): paleobiology and phylogeny. Journal of Vertebrate Paleontology 30(5): 1515–1527. doi:10.1080/02724634.2010.501437

Abello, M.A.; Rubilar-Rogers, D. 2012. Revisión del género *Abderites* Ameghino, 1887 (Marsupialia, Paucituberculata). Ameghiniana 49(2): 164–184.

Abello, M.A.; Martin, G.M.; Cardoso, Y. 2021. Review of the extinct 'shrew-opossums' (Marsupialia: Caenolestidae), with descriptions of two new genera and three new species

from the Early Miocene of southern South America. Zoological Journal of the Linnean Society 193(2): 464–498. doi:10.1093/zoolinnean/zlaa165

Abello, M.A.; Toledo, N.; Ortiz-Jaureguizar, E. 2020. Evolution of South American Paucituberculata (Metatheria: Marsupialia): adaptive radiation and climate changes at the Eocene- Oligocene boundary. Historical Biology, doi:10.1080/08912963.2018.1502286

Alvim, A.M.V.; Santos, R.V.; Roddaz, M.; Antoine, P.-O.; Ramos, M.I.F.; do Carmo, D.A.; Linhas, A.P.; Negri, F.R. 2021. Fossil isotopic constraints (C, O and 87Sr/86Sr) on Miocene shallow-marine incursions in Amazonia. Palaeogeography, Palaeoclimatology, Palaeoecology 573(1): 110422. doi:10.1016/j.palaeo.2021.110422

Anderson, V.J.; Horton, B.K.; Saylor, J.E.; Mora, A.; Tesón, E.; Breecker, D.O.; Ketcham, R.A. 2016. Andean topographic growth and basement uplift in southern Colombia: Implications for the evolution of the Magdalena, Orinoco, and Amazon river systems. Geosphere 12(4): 1235–1256. doi:10.1130/GES01294.1

Antoine, P.-O.; Salas-Gismondi, R.; Pujos, F.; Ganerød, M.; Marivaux, L. 2017. Western Amazonia as a hotspot of mammalian biodiversity throughout the Cenozoic. Journal of Mammalian Evolution 24(1): 5–17. doi:10.1007/s10914-016-9333-1

Antoine, P.-O.; Roddaz, M.; Brichau, S.; Tejada-Lara, J.; Salas-Gismondi, R.; Altamirano, A.; Louterbach, M.; Lambs, L.; Otto, T.; Brusset, S. 2013. Middle Miocene vertebrates from the Amazonian Madre de Dios Subandean Zone, Perú. Journal of South American Earth Sciences 42: 91–102. doi:10.1016/j.jsames.2012.07.008

Antoine, P.-O.; *et al*. 2016. A 60-million-year Cenozoic history of western Amazonian ecosystems in Contamana, Eastern Peru. Gondwana Research 31: 30–59. doi:10.1016/j.gr.2015.11.001

Antoine, P.-O.; *et al*. 2021. Biotic community and landscape changes around the Eocene–Oligocene transition at Shapaja, Peruvian Amazonia: regional or global drivers? Global and Planetary Change 202: 103512. doi:10.1016/j.gloplacha.2021.103512

Arnal, M.; Pérez, M.E.; Medina, L.T.; Campbell, K.E. 2022. The high taxonomic diversity of the Palaeogene hystricognath rodents (Caviomorpha) from Santa Rosa (Peru, South America) framed within a new geochronological context, Historical Biology aop. doi:10.1080/08912963.2021.2017916

Arnal, M.; Kramarz, A.G.; Vucetich, M.G.; Frailey, C.D.; Campbell, K.E. 2020. New Palaeogene caviomorphs (Rodentia, Hystricognathi) from Santa Rosa, Peru: systematics, biochronology, biogeography and early evolutionary trends. Papers in Palaeontology 6: 193–216. doi:10.1002/spp2.1264

Bahlburg, H.; Vervoort, J.D.; Du Frane, S.A.; Bock, B.; Augustsson, C.; Reimann, C. 2009. Timing of crust formation and recycling in accretionary orogens: insights learned from the western margin of South America. Earth Science Reviews 97(1–4): 215–241. doi:10.1016/j.earscirev.2009.10.006.

Bahlburg, H.; Vervoort, J.D.; DuFrane, A.; Carlotto, V.; Reimann, C.; Cárdenas, J. 2011. The U-Pb and Hf isotope evidence of detrital zircons of the Ordovician Ollantaytambo Formation, southern Peru, and the Ordovician provenance and paleogeography of southern Peru and northern Bolivia. Journal of South American Earth Sciences 32: 196–209. doi:10.1016/j.jsames.2011.07.002.

Beck, R.M.D.; Taglioretti, M.L. 2020. A nearly complete juvenile skull of the marsupial *Sparassocynus derivatus* from the Pliocene of Argentina, the affinities of Sparassocynids", and the diversification of opossums (Marsupialia; Didelphimorphia; Didelphidae). Journal of Mammalian Evolution 27: 385–417. doi:10.1007/s10914-019-09471-y

Beck, R.M.D.; Voss, R.S.; Jansa, S.A. 2021. Craniodental morphology and phylogeny of marsupials. Bulletin of the American Museum of Natural History: preprint.

Bissaro-Júnior, M.C.; Kerber, L.; Crowley, J.L.; Ribeiro, A.M.; Ghilardi, R.P.; Guilherme, E.; Negri, F.R.; Souza Filho, J.P.; Hsiou, A.S. 2019. Detrital zircon U–Pb geochronology constrains the age of Brazilian Neogene deposits from Western Amazonia. Palaeogeography, Palaeoclimatology, Palaeoecology 516: 64–70. doi:10.1016/j.palaeo.2018.11.032.

Blisniuk, P.M.; Stern, L.A.; Page Chamberlain, C.; Idleman, B.; Zeitler, P.K. 2005. Climatic and ecologic changes during Miocene surface uplift in the Southern Patagonian Andes. Earth and Planetary Science Letters 230(1–2): 125–142. doi:10.1016/j.epsl.2004.11.015.

Boivin, M.; Marivaux, L.; Orliac, M.J.; Pujos, F.; Salas-Gismondi, R.; Tejada-Lara, J.V.; Antoine, P.-O. 2017a. Late middle eocene caviomorph rodents from Contamana, Peruvian Amazonia. Palaeontologia Electronica 20.1.19A: 1–50. doi:10.26879/742

Boivin, M.; Marivaux, L.; Candela, A.M.; Orliac, M.J.; Pujos, F.; Salas-Gismondi, R.; Tejada-Lara, J.V.; Antoine P.-O. 2017b. Late Oligocene caviomorph rodents from Contamana, Peruvian Amazonia. Papers in Palaeontology 3(1): 69–109. doi:10.1002/spp2.1068

Boivin, M.; Marivaux, L.; Pujos, F.; Salas-Gismondi, R.; Tejada-Lara, J.V.; Varas-Malca, R. M.; Antoine, P.-O. 2018. Early Oligocene caviomorph rodents from Shapaja, Peruvian Amazonia. Palaeontographica 311(1–6): 87–156. doi:10.1127/pala/2018/0075

Boivin, M.; *et al*. 2021. Late middle Miocene caviomorph rodents from Tarapoto, Peruvian Amazonia. PLoS ONE 16(11): e0258455. doi:10.1371/journal.pone.0258455

Boonstra, M.; Ramos, M.I.F.; Lammertsma, E.I.; Antoine, P.-O.; Hoorn, C. 2015. Marine connections of Amazonia: evidence from foraminifera and dinoflagellate cysts (early to middle Miocene, Colombia/Peru). Palaeogeography, Palaeoclimatology, Palaeoecology 417: 176–194. doi:10.1016/j.palaeo.2014.10.032

Bown, T.M.; Fleagle, J.G. 1993. Systematics, biostratigraphy, and dental evolution of the Palaeothentidae, later Oligocene to early-middle Miocene (Deseadan-Santacrucian) caenolestoid marsupials of South America. Journal of Paleontology 67(29): 1–76. doi:10.1017/S0022336000062107

Bühn, B.; Pimentel, M.M.; Matteini, M.; Dantas, E.L. 2009. High spatial resolution analysis of Pb and U isotopes for geochronology by laser ablation multi-collector inductively coupled plasma mass spectrometry (LA-MC-ICP-MS). Anais da Academia Brasileira de Ciências 81(1): 99–114. doi:10.1590/S0001-37652009000100011

Cadena, E.A.; Anaya, F.; Croft, D.A. 2015. Giant fossil tortoise and freshwater chelid turtle remains from the middle Miocene, Quebrada Honda, Bolivia: evidence for lower paleoelevations for the southern Altiplano. Journal of South American Earth Sciences 64(1): 190–198. doi:10.1016/j.jsames.2015.10.013

Carvalho, M.R.; *et al*. 2021. Extinction at the end-Cretaceous and the origin of modern Neotropical rainforests. Science 372(6537): 63–68. doi:10.1126/science.abf1969

Castro, M.C.; Dahur, M.J.; Ferreira, G.S. 2021. Amazonia as the origin and diversification area of Didelphidae (Mammalia: Metatheria), and a review of the fossil record of the clade. Journal of Mammalian Evolution 28: 583–598. doi:10.1007/s10914-021-09548-7

Chew, D.M.; Schaltegger, U.; Košler, J.; Whitehouse, M.J.; Gutjahr, M.; Spikings, R.A.; Miškovic, A. 2007. U-Pb geochronologic evidence for the evolution of the Gondwanan margin of the north-central Andes. Geological Society of America Bulletin 119(5–6): 697–711. doi:10.1130/B26080.1

Chew, D.M.; Magna, T.; Kirkland, C.L.; Mišković, A.; Cardona, A.; Spikings, R.; Schaltegger, U. 2008. Detrital zircon fingerprint of the Proto-Andes: evidence for a Neoproterozoic active margin? Precambrian Research 167(1): 186–200. doi:10.1016/j.precamres.2008.08.002.

Chornogubsky, L.; Kramarz, A.G. 2012. Nuevos hallazgos de Microbiotheriidae (Mammalia, Marsupialia) en la Formación Pinturas (Mioceno temprano, Argentina). Ameghiniana 49(4): 442–450.

Cozzuol, M.A.; Goin, F.; de los Reyes, M.; Ranzi, A. 2006. The oldest species of *Didelphis* (Mammalia, Marsupialia, Didelphidae), from the late Miocene of Amazonia. Journal of Mammalogy 87(4): 663–667. doi:10.1644/05-MAMM-A-282R2.1

Croft, D.A. 2007. The middle Miocene (Laventan) Quebrada Honda fauna, southern Bolivia and a description of its notoungulates. Palaeontology 50(1): 277–303. doi:10.1111/j.1475-4983.2006.00610.x

Croft, D.A. 2016. Horned armadillos and rafting monkeys. Indiana University Press: 304 p. Bloomington and Indianopolis.

Croft, D.A.; Engelman, R.K.; Dolgushina, T.; Wesley, G. 2018. Diversity and disparity of sparassodonts (Metatheria) reveal non-analogue nature of ancient South American mammalian carnivore guilds. Proceedings of the Royal Society B 285: 20172012. doi:10.1098/rspb.2017.2012

Croft, D.A.; Carlini, A.A.; Ciancio, M.R.; Brandoni, D.; Drew, N.E.; Engelman, R.K.; Anaya, F. 2016. New mammal faunal data from Cerdas, Bolivia, a middle-latitude Neotropical site that chronicles the end of the Middle Miocene Climatic Optimum in South America. Journal of Vertebrate Paleontology 36(5): e1163574. doi:10.1080/02724634.2016.1163574

Czaplewski, N.J. 1996. Opossums (Didelphidae) and bats (Noctilionidae and Molossidae) from the late Miocene of the Amazon Basin. Journal of Mammalogy 77(1): 84–94. doi:10.2307/1382711

Defler, T. 2019. History of Terrestrial Mammals in South America. Springer: 372 p. Cham.

Deschamps, C.M.; Tonni, E.P. 1992. Los vertebrados del Pleistoceno tardío-Holoceno del Arroyo Naposta Grande, Provincia de Buenos Aires: aspectos paleoambientales. Ameghiniana 29(3): 201–210.

Dickinson, W.R.; Gehrels, G.E. 2009. Use of U-Pb ages of detrital zircons to infer maximum depositional ages of strata: a test against a Colorado Plateau Mesozoic database. Earth and Planetary Science Letters 288(1–2): 115–125. doi:10.1016/j.epsl.2009.09.013

Dumont, E.R.; Bown, T.M. 1997. New caenolestoid marsupials. *In* Vertebrate Paleontology in the Neotropics. The Miocene fauna of La Venta, Colombia (Kay, R.F.; Madden, R.H.; Cifelli, R.L.; Flynn, J.J.; editors). Smithsonian Institution Press: 207–212. Washington and London.

Dumont, E.; Strait, S.; Friscia, A. 2000. Abderitid marsupials from the Miocene of Patagonia: an assessment of form, function, and evolution. Journal of Paleontology 74(6): 1161–1172. doi:10.1666/0022-3360(2000)0742.0.CO;2

Engelman, R.K.; Anaya, F.; Croft, D.A. 2015. New specimens of *Acyon myctoderos* (Metatheria, Sparassodonta) from Quebrada Honda, Bolivia. Ameghiniana 52: 204–225. doi:10.5710/AMGH.19.11.2014.2803

Engelman, R.K.; Anaya, F.; Croft, D.A. 2017. New palaeothentid marsupials (Paucituberculata) from the middle Miocene of Quebrada Honda, Bolivia, and their implications for the palaeocology, decline and extinction of the Palaeothentoidea. Journal of Systematic Palaeontology 15(10): 787–820. doi:10.1080/14772019.2016.1240112

Engelman, R.K.; Anaya, F.; Croft, D.A. 2020. *Australogale leptognathus*, gen. et sp. nov., a second species of small sparassodont (Mammalia: Metatheria) from the Middle Miocene locality of Quebrada Honda, Bolivia. Journal of Mammalian Evolution 27(1): 37–54. doi:10.1007/s10914-018-9443-z

Erlich, R.N.; Fallon, J.; O'Sullivan, P. 2018. Stratigraphy and LA-ICP-MS zircon U-Pb provenance of middle Permian to Maastrichtian sandstones from outcrop and subsurface control in the sub-Andean basins of Peru. *In* Petroleum basins and hydrocarbon potential of the Andes of Peru and Bolivia (Zamora, G.; McClay, K.R.; Ramos, V.A.; editors). AAPG Memoir 117: 175–222.

Eude, A.; Roddaz, M.; Brichau, S.; Brusset, S.; Calderon, Y.; Baby, P.; Soula, J.-C. 2015. Controls on timing of exhumation and deformation in the northern Peruvian eastern Andean wedge as inferred from low-temperature thermochronology and balanced cross section. Tectonics 34(4): 715–730. doi:10.1002/2014TC003641

Fleagle, J.G.; Kay, R.F.; Anthony, M.R.L. 1997. Fossil New World Monkeys. *In* Vertebrate Paleontology in the Neotropics. The Miocene fauna of La Venta, Colombia (Kay, R.F.; Madden, R.H.; Cifelli, R.L.; Flynn, J.J.; editors). Smithsonian Institution Press: 473–495. Washington and London.

Flynn, J.J.; Charrier, R.; Croft, D.A.; Wyss, A.R. 2012. Cenozoic Andean faunas: shedding new light on South American mammal evolution, biogeography, environments, and tectonics. *In* Bones, clones, and biomes: the history and geography of recent neotropical mammals (Patterson, B.D.; Costa, L.P.; editors). The University of Chicago Press: 51–75. Chicago and London.

Frailey, C.D.; Campbell, K.E. 2004. Paleogene rodents from Amazonian Peru: the Santa Rosa local fauna. *In* The Paleogene mammalian fauna of Santa Rosa, Amazonian Peru (Campbell, K.E.; editor). Natural History Museum of Los Angeles County, Science Series 40: 71–130. Los Angeles.

Gardner, A.L. 2007. Mammals of South America. Vol. 1. The University of Chicago Press: 669 p. Chicago.

Garreaud, R.D. 2009. The Andes climate and weather. Advances in Geosciences 22: 3–11. doi:10.5194/adgeo-22-3-2009, 2009.

Gehrels, G. 2014. Detrital zircon U-Pb geochronology applied to tectonics. Annual Review of Earth and Planetary Sciences 42: 127–149. doi:10.1146/annurev-earth-050212-124012

Gehrels, G.E.; Valencia, V.A.; Ruiz, J. 2008. Enhanced precision, accuracy, efficiency, and spatial resolution of U-Pb ages by laser ablation-multicollector-inductively coupled plasma-mass spectrometry. Geochemistry, Geophysics, Geosystems 9(3): 1–13. doi:10.1029/2007GC001805

Gibert, L.; Deino, A.; Valero, L.; Anaya, F.; Lería, M.; Saylor, B.; Croft, D.A. 2020. Chronology of Miocene terrestrial deposits and fossil vertebrates from Quebrada Honda (Bolivia). Palaeogeography, Palaeoclimatology, Palaeoecology 560: 110013. doi:10.1016/j.palaeo.2020.110013

Goillot, C.; Antoine, P.-O.; Tejada, J.; Pujos, F.; Salas Gismondi, R. 2011. Middle Miocene Uruguaytheriinae (Mammalia, Astrapotheria) from Peruvian Amazonia and a review of the astrapotheriid fossil record in northern South America. Geodiversitas 33(2): 331–345. doi:10.5252/g2011n2a8

Goin, F.J. 1997. New clues for understanding Neogene marsupial radiations. *In* Vertebrate Paleontology in the Neotropics. The Miocene fauna of La Venta, Colombia (Kay, R.F.; Madden, R.H.; Cifelli, R.L.; Flynn, J.J.; editors). Smithsonian Institution Press: 187–206. Washington and London.

Goin, F.J.; Abello, M.A. 2013. Los Metatheria sudamericanos de comienzos del Neógeno (Mioceno Temprano, Edad–Mamífero Colhuehuapense). Parte II: Microbiotheria y Polydolopimorphia. Ameghiniana 50(1): 51–78.

Goin, F.J.; Candela, A.M. 2004. New Palaeogene marsupials from the Amazon Basin of Eastern Peru. *In* The Paleogene mammalian fauna of Santa Rosa, Amazonian Peru (Campbell, K.E.; editor). Natural History Museum of Los Angeles County, Science Series 40: 15–60. Los Angeles.

Goin, F.J.; de los Reyes, M. 2011. Contribución al conocimiento de los representantes extintos de *Lutreolina* Thomas, 1910 (Mammalia, Marsupialia, Didelphidae). Historia Natural 1(2): 15–25.

Goin, F.J.; Abello, M.A.; Chornogubsky, L. 2010. Middle Tertiary marsupials from central Patagonia (early Oligocene of Gran Barranca): understanding South America's Grande

Coupure. *In* The paleontology of Gran Barranca: evolution and environmental change through the Middle Cenozoic of Patagonia (Madden, R.H.; Carlini, A.A.; Vucetich, M.G.; Kay, R.F.; editors). Cambridge University Press: 71–107. New York.

Goin, F.J.; Montalvo, C.I.; Visconti, G. 2000. Los marsupiales (Mammalia) del Mioceno Superior de la Formación Cerro Azul (Provincia de La Pampa, Argentina). Estudios Geológicos 56(1–2): 101–126.

Goin, F.J.; Case, J.A.; Woodburne, M.O. Vizcaíno, S.F.; Reguero, M.A. 1999. New discoveries of "oppossum-like" marsupials from Antarctica (Seymour Island, Medial Eocene). Journal of Mammalian Evolution 6: 335–365. doi:10.1017/S0954102094000027

Goin, F.J.; Woodburne, M.O.; Zimicz, A.N.; Martin, G.M.; Chornogubsky, L. 2016. A Brief History of South American Metatherians. Evolutionary Contexts and Intercontinental Dispersals. Springer Earth System Sciences: 237 p. New York.

Goin, F.J.; Abello, A.; Bellosi, E.; Kay, R.; Madden, R.; Carlini, A. 2007. Los Metatheria sudamericanos de comienzos del Neógeno (Mioceno Temprano, Edad-mamífero Colhuehuapense). Parte I: Introducción, Didelphimorphia y Sparassodonta. Ameghiniana 44(1): 29–71.

Hadler, P.; Ferigolo, J.; Goin, F.J. 2009. Mamíferos de pequeno porte (Didelphimophia, Chiroptera e Rodentia) do Pleistoceno Final/Holoceno do Brasil, com ênfase no Rio Grande do Sul. *In* Quaternário do Rio Grande do Sul: integrando conhecimentos (Ribeiro, A.M.; Bauermann, S.G.; Scherer, C.S.; editors). Sociedade Brasileira de Paleontologia: 155–170. Porto Alegre.

Hartwig, W.C.; Meldrum, D.J. 2002. Miocene platyrrhines of the northern Neotropics. *In* The Primate Fossil Record (Hartwig, W.C.; editor). Cambridge University Press: 175–188. Cambridge.

Hoorn, C.; *et al*. 2010. Amazonia through time: Andean uplift, climate change, landscape evolution, and biodiversity. Science 330(6006): 927–931. doi:10.1126/science.1194585

Hungerbühler, D.; Steinmann, M.; Winkler, W.; Seward, D.; Egüez, A.; Peterson, D.E.; Helg, U.; Hammer, C. 2002. Neogene stratigraphy and Andean geodynamics of southern Ecuador. Earth-Science Reviews 57(1): 75–124. doi:10.1016/S0012-8252(01)00071-X

Hurtado, C.; Roddaz, M.; Santos, R.V.; Baby, P.; Antoine, P.-O.; Dantas, E.L. 2018. Cretaceous-early Paleocene drainage shift of Amazonian rivers driven by Equatorial Atlantic Ocean opening and Andean uplift as deduced from the provenance of northern Peruvian sedimentary rocks (Huallaga basin). Gondwana Research 63: 152–168. doi:10.1016/j.gr.2018.05.012

Jansa, S.A.; Barker, F.K.; Voss, R.S. 2014. The early diversification history of didelphid marsupials: a window into South America's "splendid isolation." Evolution 68: 684–695. doi:10.1111/Evo.12290

Jaramillo, C.; Hoorn, C.; Silva, S.A.F.; Leite, F.; Herrera, F.; Quiroz, L.; Dino, R.; Antonioli, L. 2010. The origin of the modern Amazon rainforest: implications of the palynological and palaeobotanical record. *In* Amazonia: landscape and species evolution (Hoorn, C.; Wesselingh, F.P.; editors). Wiley□Blackwell Publishing Ltd: 317–334. London.

Jaramillo, C.; *et al*. 2017. Miocene flooding events of western Amazonia. Science Advances 3: e1601693. doi:10.1126/sciadv.1601693

Jiménez-Lara, K. 2020. Systematic revision and redefinition of the genus *Scirrotherium* Edmund and Theodor, 1997 (Cingulata, Pampatheriidae): Implications for the origin of pampatheriids and the evolution of the South American lineage including *Holmesina*. Geobios 62: 1–21. doi:10.1016/j.geobios.2020.07.002.

Kay, R.F. 2015. Biogeography in deep time - What do phylogenetics, geology, and paleoclimate tell us about early platyrrhine evolution? Molecular Phylogenetics and Evolution 82: 358–374. doi:10.1016/j.ympev.2013.12.002

Kay, R.F.; Madden, R.H. 1997. Mammals and rainfall: Paleoecology of the middle Miocene at la Venta (Colombia, South America). Journal of Human Evolution 32(2–3): 161–199. doi:10.1006/jhev.1996.0104

Kay, R.F.; Madden, R.H.; Cifelli, R.L.; Flynn, J.J. 1997. Vertebrate Paleontology in the Neotropics: The Miocene Fauna of La Venta, Colombia. Smithsonian Institution Press: 592 p. Washington.

Kramarz, A.G.; Bellosi, E.S. 2005. Hystricognath rodents from the Pinturas Formation, Early–Middle Miocene of Patagonia, biostratigraphic and paleoenvironmental implications. Journal of South American Earth Sciences 18(2): 199–212. doi:10.1016/j.jsames.2004.10.005

Linares, O.J. 2004. Bioestratigrafía de la fauna de mamíferos de las formaciones Socorro, Urumaco y Codore (Mioceno Medio-Plioceno Temprano) de la región de Urumaco, Falcon, Venezuela. Paleobiologia Neotropical 1: 1–26.

Litty, C.; Lanari, P.; Burn, M.; Schlunegger, F. 2017. Climate-controlled shifts in sediment provenance inferred from detrital zircon ages, western Peruvian Andes. Geology 45(1): 59–62. doi:10.1130/G38371.1

Louterbach, M.; *et al*. 2018. Provenance record of late Maastrichtian–late Palaeocene Andean Mountain building in the Amazonian retroarc foreland basin (Madre de Dios basin, Peru). Terra Nova 30(1): 17–23. doi:10.1111/ter.12303

Madden, R.H.; Guerrero, J.; Kay, R.F.; Flynn, J.J.; Swisher III, C.C.; Walton, A.H. 1997. The Laventan stage and age. *In* Vertebrate Paleontology in the Neotropics. The Miocene fauna of La Venta, Colombia (Kay, R.F.; Madden, R.H.; Cifelli, R.L.; Flynn, J.J.; editors). Smithsonian Institution Press: 499–519. Washington and London.

Magurran, A.E. 2004. Measuring biological diversity. Blackwell Publishing: 256 p. Oxford.

Marivaux, L.; Adnet, S.; Altamirano-Sierra, A.J.; Pujos, F.; Ramdarshan, A.; Salas-Gismondi, R.; Tejada-Lara, J.V.; Antoine, P.-O. 2016a. Dental remains of cebid platyrrhines from the earliest late Miocene of Western Amazonia, Peru: macroevolutionary implications on the extant capuchin and marmoset lineages. American Journal of Physical Anthropology 161(3): 478–493. doi:10.1002/ajpa.23052

Marivaux, L.; Adnet, S.; Altamirano-Sierra, A.J.; Boivin, M.; Pujos, F.; Ramdarshan, A.; Salas-Gismondi, R.; Tejada-Lara, J.V.; Antoine, P.-O. 2016b. Neotropics provide insights into the emergence of New World monkeys: new dental evidence from the late Oligocene of Peruvian Amazonia. Journal of Human Evolution 97: 159–175. *doi:10.1016/j.jhevol.2016.05.011*

Marivaux, L.; Aguirre-Dias, W.; Benites-Palomino, A.; Billet, G.; Boivin, M.; Pujos, F.; Salas-Gismondi, R.; Tejada-Lara, J.V.; Varas-Malca, R.M.; Antoine, P.-O. 2020. New record of *Neosairimi* (Cebidae, Platyrrhini) from the late Middle Miocene of Peruvian Amazonia. Journal of Human Evolution 146: 102835. doi:10.1016/j.jhevol.2020.102835

Marshall, L.G. 1976. New Didelphine marsupials from the La Venta fauna (Miocene) of Colombia, South America. Journal of Paleontology 50(3): 402–418.

Montes, C.; *et al*. 2021. A Middle to Late Miocene trans-andean portal: geologic record in the Tatacoa Desert. Frontiers in Earth Science 8: 587022. doi:10.3389/feart.2020.587022

Moreno, F.; Garzione, C.N.; George, S.W.M.; Horton, B.K.; Williams, L.; Jackson, L.J.; Carlotto, V.; Richter, F.; Bandeian, A. 2020. Coupled Andean growth and foreland basin evolution, Campanian–Cenozoic Bagua Basin, northern Peru. Tectonics 39(7): e2019TC005967. doi:10.1029/2019TC005967

Moreno, F.; *et al*. 2015. Revised stratigraphy of Neogene strata in the Cocinetas Basin, La Guajira, Colombia. Swiss J Palaeontol 134: 5–43. doi:10.1007/s13358-015-0071-4

Motta, F.A.; Hadler, P.; Cherem, J.J.; Ribeiro, A.M. 2019. A marsupial assemblage (Mammalia, Didelphimorphia) from the Quaternary of the Serra da Capivara, State of

Piauí, Brazil. Revista Brasileira de Paleontologia 22(3): 225–239. doi:10.4072/rbp.2019.3.05

Navarro, P.; Rivera, M.; Monge, R. 2010. Geología y metalogenia del Grupo Calipuy (volcanismo Cenozoico) segmento Santiago de Chuco, norte del Perú. INGEMMET, Boletín, Serie D, Estudios Regionales, 28: 202 p. Lima.

Negri, F.R.; Bocquentin-Villanueva, J.; Ferigolo, J.; Antoine, P.-O. 2010. A review of Tertiary mammal faunas and birds from Western Amazonia. *In* Amazonia: landscape and species evolution: a look into the past (Hoorn, C.; Wesselingh, F.P; editors). Wiley Blackwell Publishing Ltd: 243–258. London.

Prevosti, F.J.; *et al*. 2021. New radiometric 40Ar–39Ar dates and faunistic analyses refine evolutionary dynamics of Neogene vertebrate assemblages in Southern South America. Scientific Reports 11: 9830. doi:10.1038/s41598-021-89135-1

Quintero-Galvis, J.F.; Saenz-Agudelo, P.; Celis-Diez, J.L.; Amico, G.C.; Vazquez, S.; Shafer, A.B.; Nespolo, R.F. 2021. The biogeography of *Dromiciops* in Southern South America: middle Miocene transgressions, speciation and associations with *Nothofagus*. Molecular Phylogenetics and Evolution 163: 107234. doi:10.1016/j.ympev.2021.107234

Quiroz, L.; Jaramillo, C. 2010. Stratigraphy and sedimentary environments of Miocene shallow to marginal marine deposits in the Urumaco Through, Falcón Basin, western Venezuela. *In* Urumaco and Venezuelan Paleontology: The Fossil Record of the Northern Neotropics (Sánchez-Villagra, M.R.; Aguilera, O.; Carlini, A.A.; editors). Indiana University Press: 153–172. Bloomington.

Raffi, I.; Wade, B.S.; Pälike, H.; Beu, A.G.; Cooper, R.; Crundwell, M.P. *et al*. 2020. Chapter 29 – The Neogene Period. *In* Geologic Time Scale 2020. Vol. 2. (Gradstein, F.M.; Ogg, J.G.; Schmitz, M.D.; Ogg, G.M.; editors). Elsevier: 1141–1215. Amsterdam.

Rincón, A.D.; Solórzano, A.; Benammi, M.; Vignaud, P.; McDonald, H.G. 2014. Chronology and geology of an Early Miocene mammalian assemblage in North of South America, from Cerro La Cruz (Castillo Formation), Lara state, Venezuela: implications in the ‘changing course of Orinoco River’ hypothesis. Andean Geology 41(3): 507–528. doi:10.5027/andgeoV41n3-a02

Roddaz, M.; Hermoza, W.; Mora, A.; Baby, P.; Parra, M.; Christophoul, F.; Brusset, S.; Espurt, N. 2010. Cenozoic Sedimentary Evolution of the Amazonian Foreland Basin System. *In* Amazonia: Landscape and Species Evolution: a Look into the Past (Hoorn, C.; Wesselingh, F.P; editors). Wiley Blackwell Publishing Ltd: 61–88. London.

Rosenberger, A.L.; Hartwig, W.C. 2013. New World Monkeys. *In* eLS. John Wiley & Sons, Ltd (editor). doi:10.1002/9780470015902.a0001562.pub3

Salas-Gismondi, R.; Flynn, J.J.; Baby, P.; Tejada-Lara, J.; Wesselingh, F.P.; Antoine, P.-O. 2015. A Miocene hyperdiverse crocodylian community reveals peculiar trophic dynamics in proto-Amazonian megawetlands. Proceedings of the Royal Society B: Biological Sciences 282(1804): 20142490. doi:10.1098/rspb.2014.2490

Sánchez-Villagra, M.R.; Aguilera, O.A.; Sánchez, R.; Carlini, A.A. 2010. The fossil vertebrate record of Venezuela of the last 65 million years. *In* Urumaco and Venezuelan Paleontology: The Fossil Record of the Northern Neotropics (Life of the Past) (Sánchez-Villagra, M.R.; Aguilera, O.A.; Carlini, A.A.; editors). Indiana University Press: 19–51. Bloomington.

Sato, K.; Teixeira, W.; Tassinari, C.; Basei, M. 2000. Crustal evolution of the South American platform. *In* Tectonic Evolution of South America (Cordani, U.; Milani, E.J.; Tomaz Filho, A.; Campos, D.A.; editors). 31st International Geological Congress: 19–40. Rio de Janeiro.

Sharman, G.R.; Malkowski, M.A. 2020. Needles in a haystack: detrital zircon U-Pb ages and the maximum depositional age of modern global sediment. Earth-Science Reviews 203: 103109. doi:10.1016/j.earscirev.2020.103109

Sharman, G.R.; Sharman, J.P.; Sylvester, Z. 2018. detritalPy: a Python-based toolset for visualizing and analyzing detrital geo-thermochronologic data. The Depositional Record 4(2): 202–215. doi:10.1002/dep2.45

Spikings, R.; Reitsma, M.J.; Boekhout, F.; Mišković, A.; Ulianov, A.; Chiaradia, M.; Gerdes, A.; Schaltegger, U. 2016. Characterization of Triassic rifting in Peru and implications for the early disassembly of western Pangaea. Gondwana Research 35:124–143. doi:10.1016/j.gr.2016.02.008.

Spradley, J.P.; Glazer, B.J.; Kay, R.F. 2019. Mammalian faunas, ecological indices, and machine-learning regression for the purpose of paleoenvironment reconstruction in the Miocene of South America. Palaeogeography, Palaeoclimatology, Palaeoecology 518: 155–171. doi:10.1016/j.palaeo.2019.01.014

Stutz, N.S.; *et al*. 2021. Neotropical metatherian diversity around the Eocene-Oligocene transition: the Shapaja section, Peruvian Amazonia. Libro de Resúmenes – 14 CAPA, Symposium Mamíferos del Paleógeno de América del Sur: 123.

Suárez, C.; Forasiepi, A.; Goin, F.J.; Jaramillo, C. 2016. Insights into the Neotropics prior to the Great American Biotic Interchange: new evidence of mammalian predators from the

Miocene of Northern Colombia. Jounal of Vertebrate Paleontology 36(1): e1029581. doi:10.1080/02724634.2015.1029581

Suárez Gómez, C. 2019. Estudios Taxonómicos y Paleobiológicos sobre los Metatheria (Mammalia) del Mioceno Medio de La Venta, Colombia. Ph.D. thesis (Unpublished), Universidad Nacional de la Plata: 292 p.

Tejada-Lara, J.; Salas-Gismondi, R.; Pujos, F.; Baby, P.; Benammi, M.; Brusset, S.; Franceschi, D.; Espurt, N.; Urbina, M.; Antoine, P.-O. 2015. Life in Proto-Amazonia: Middle Miocene mammals from the Fitzcarrald Arch (Peruvian Amazonia). Palaeontology 58(2): 341–378. doi:10.1111/pala.12147

Verzi, D.H.; Montalvo, C.I.; Deschamps, C.M. 2008. Biostratigraphy and biochronology of the Late Miocene of central Argentina: evidence from rodents and taphonomy. Geobios 41(1): 145–155. doi:10.1016/j.geobios.2006.09.005

Villarroel, C.; Marshall, L.G. 1983. Two New Late Tertiary Marsupials (Hathlyacyninae and Sparassocyninae) from the Bolivian Altiplano. Journal of Paleontology 57(5): 1061-1066.

Voss, R.S.; Jansa, S.A. 2009. Phylogenetic relationships and classification of didelphid marsupials, an extant radiation of New World metatherian mammals. Bulletin of the American Museum of Natural History 322: 1–177.

Voss, R.S.; Jansa, S.A. 2021. Opossums: an Adaptive Radiation of New World Marsupials. John Hopkins University Press: 328 p. Baltimore.

Westerhold, T.; *et al*. 2020. An astronomically dated record of Earth's climate and its predictability over the last 66 million years. Science 369(6509): 1383–1388. doi:10.1126/science.aba6853

Wing, S.L.; Herrera, F.; Jaramillo, C.A.; Gómez-Navarro, C.; Wilf, P.; Labandeira, C.C. 2009. Late Paleocene fossils from the Cerrejón Formation, Colombia, are the earliest record of neotropical rainforest. Proceedings of the National Academy of Sciences 106(44): 18627–18632. doi: 10.1073/pnas.0905130106